The RhoGEF protein Plekhg5 regulates apical constriction of bottle cells during gastrulation

Ivan K. Popov[1], Heather J. Ray[1], Paul Skoglund[2], Ray Keller[2], and Chenbei Chang[1, *]

[1]Department of Cell, Developmental, and Integrative Biology
University of Alabama at Birmingham
Birmingham, AL 35294
USA

[2]Biology Department
University of Virginia
Charlottesville, VA 22903
USA

* Corresponding author
cchang@uab.edu

Summary Statement

This study demonstrates that a RhoGEF expressed in the bottle cells of Xenopus gastrulae is recruited to the apical cell cortex in a PH- and GEF-dependent manner and promotes apical actomyosin activity to control apical constriction during gastrulation.

Abstract

Apical constriction regulates epithelial morphogenesis during embryonic development, but how this process is controlled is not understood completely. Here, we identify a Rho guanine nucleotide exchange factor (GEF) *plekhg5* as an essential regulator of apical constriction of bottle cells during *Xenopus* gastrulation. *plekhg5* is expressed in the blastopore lip and its expression is sufficient to induce ectopic bottle cells in epithelia of different germ layers in a Rho-dependent manner. This activity is not shared by *arhgef3*, another organizer-specific RhoGEF. Plekhg5 protein is localized in the apical cell cortex via its PH domain, and the GEF activity enhances its apical recruitment. Plekhg5 induces apical actomyosin accumulation and cell elongation. Knockdown of *plekhg5* inhibits activin-induced bottle cell formation and endogenous blastopore lip formation in gastrulating frog embryos. Apical accumulation of actomyosin, apical constriction, and bottle cell formation fail to occur in these embryos. Taken together, our data indicate that transcriptional regulation of *plekhg5* expression at the blastopore lip determines bottle cell morphology via local polarized activation of Rho by Plekhg5 which stimulates apical actomyosin activity to induce apical constriction.

Key Words: Apical constriction, bottle cell, gastrulation, RhoGEF, actin, myosin

Introduction

Apical constriction refers to an active reduction of cell apical surface area that then causes further cell shape changes, such as elongation of cells along the apical-basal axis and/or expansion of the basolateral cell compartment. Apical constriction can drive bending of epithelial cell sheets, generate lumens and tubes, facilitate cell ingression and tissue invagination, and promote epithelial-to-mesenchymal transition. Apical constriction is thus a central mechanism underlying epithelial morphogenesis during multiple developmental contexts, such as gastrulation, neural tube closure, and sensory organ formation (reviewed in Sawyer et al., 2010). In adults, apical constriction is also utilized in distinct conditions, such as wound healing. The reiterative usage of apical constriction in various tissue contexts highlights the importance of understanding the cellular and the molecular mechanisms controlling this fundamental process.

One common theme emerging from studies of apical constriction in different tissue contexts in a wide range of animal models is that polarized positioning and activation of actomyosin cytoskeleton within the constricting cells is crucial (reviewed in Martin and Goldstein, 2014). Both F-actin assembly and myosin accumulation and activation occur preferentially in the apical cell cortex prior to apical constriction, and contractile forces generated by this apical actomyosin decreases apical cell surface area (Martin et al., 2009; Ebrahim et al., 2012; Mason et al., 2013). The polarized assembly of the cytoskeleton network near the apical cell membrane must be tightly controlled, both temporally and spatially, for the coordinated individual cell shape changes that drive global tissue morphogenesis to occur (Martin and Goldstein, 2014). Rho family of small GTPases have often been implicated in such precise control of actomyosin dynamics during apical constriction.

The main members of the Rho family GTPases include RhoA, Rac1 and Cdc42. All of them are involved in regulation of actomyosin cytoskeleton, though they exert differential effects on the structure and the dynamics of the actomyosin cytoskeleton. In mammalian cells, RhoA preferentially controls stress fiber and focal adhesion formation, whereas Rac1 and Cdc42 are associated mainly with lamellipodia and filopodia protrusions, respectively (Hall 1998). The Rho proteins switch between a GTP-bound active state and a GDP-bound inactive state. The conversion between the two states is regulated by guanine nucleotide exchange factors (GEFs),

which catalyze the exchange of GDP for GTP to activate Rho proteins, and GTPase-activating proteins (GAPs), which enhance the low intrinsic GTPase activity of Rho members to inactivate them. GEFs and GAPs respond to various intra- and inter-cellular signals to control diverse functions of Rho proteins, such as cell division, differentiation and movements (Hodge and Ridley, 2016). Rho members as well as their GEF and GAP regulators have been shown to regulate apical constriction. During *Drosophila* gastrulation, a Rho-specific GEF, DRhoGEF2, is enriched apically in invaginating ventral furrow cells, regulates apical myosin II accumulation and F-actin assembly, and is required for RhoA-dependent cell shape changes and normal tissue invagination (Barrett et al., 1997; Hacker and Perrimon, 1998; Nikolaidou and Barrett, 2004; Barmchi et al., 2005). A requirement for RhoA-dependent apical constriction has also been described during gastrulation of sea urchin and ascidian, though the upstream Rho regulators have not been reported in these species (Beane et al., 2006; Sherrard et al., 2010). In contrast, Cdc42, but not Rho, seems to be crucial during *C. elegans* endodermal internalization at gastrulation. Cell contact-induced recruitment of a Cdc42-specific GAP, PAC-1, results in inactivation of Cdc42 at the basolateral cell membrane, leaving active Cdc42 only at the contact-free apical surface. This stimulates the activity of the Cdc42 effector MRCK-1 apically to phosphorylate and activate myosin II for apical constriction of endodermal cells (Lee and Goldstein, 2003; Anderson et al., 2008; Chan and Nance, 2013; Marston et al., 2016). Thus, apical constriction can be driven by different upstream regulators converging on regulation of the apical actomyosin cytoskeleton. Unlike the invertebrates, the GEFs and GAPs utilized during gastrulation of vertebrate embryos have not been described in detail.

During *Xenopus* gastrulation, a group of surface cells undergo apical constriction and basolateral elongation and expansion to form bottle-shaped cells. The cortical melanosomes become concentrated as the apical cell surface shrinks, hence marking the bottle cells with dark pigmentation. The bottle cells first appear on the dorsal side (known as the dorsal lip) and subsequently spread laterally and ventrally to encompass the entire blastopore (blastopore lip). Mesodermal and endodermal tissues involute through the blastopore and thereby internalize. The formation, morphology, and function of the bottle cells have been described by scanning electron microscopy and time lapse video microscopy studies decades ago (Keller 1981, Hardin and Keller, 1988), and the molecular machinery involved in this process is currently being

uncovered. It is shown that both actin and microtubule cytoskeletons regulate bottle cell formation, and endocytosis is required to remove apical cell membrane for efficient apical constriction (Lee and Harland, 2007, 2010). Upstream regulators of bottle cell formation include the activin/nodal signaling pathway, which can induce ectopic bottle cells associated with ectopic mesendoderm in the animal region (Kurth and Hausen, 2000). The components in the Wnt planar cell polarity pathway and the apical-basal polarity protein Lethal-giant-larvae (Lgl) have also been implicated in regulating bottle cell formation (Choi and Sokol, 2009; Ossipova et al., 2015). However, all these factors are expressed more broadly than at the blastopore lip. It is thus unclear how positioning of the bottle cells is regulated in gastrulating embryos and whether and which Rho GEFs or GAPs participate in controlling apical constriction of bottle cells.

In this study, we report the identification of a RhoGEF, *plekhg5*, as a blastopore lip-specific gene during *Xenopus* gastrulation. Plekhg5 protein is apically localized in epithelial cells and can organize apical actomyosin assembly. *plekhg5* induces ectopic blastopore lip-like morphology in a Rho-dependent fashion in epithelial cells, and its gene product is required for bottle cell formation in *Xenopus* embryos. Our studies thus reveal that expression of a tissue-specific RhoGEF is both necessary and sufficient to induce apical constriction required for bottle cell formation during *Xenopus* gastrulation.

Results

plekhg5 is expressed in cells at the blastopore lip during *Xenopus* gastrulation

In a previous RNA-seq study of differentially expressed genes in distinct tissues of *Xenopus* gastrulae, we identified *plekhg5* as a RhoGEF that is enriched in the organizer of early *Xenopus* embryos (Popov et al., 2017). Whole mount in situ hybridization (ISH) revealed that *plekhg5* RNA is first detected in early gastrula embryos in the dorsal lip region. Its expression then spreads to encompass the entire blastopore lip during mid-gastrulation and is down-regulated once cells involute inside the embryos and re-spread at late gastrula stages (Fig. 1a-f). Bisected embryos showed that *plekhg5* expression is limited to the surface cells at the blastopore lip (Fig. 1b, d, f). At the neurula and early tailbud stages, *plekhg5* RNA is seen in the head at the hindbrain level and the tail regions (Fig. 1g to k). This pattern of expression persists through late tailbud stages, with additional expression apparent in the otic placodes and the pharyngeal

pouches (Fig. 1l and m). Both the notochord and the dorsal neural tube in the tail region contain *plekhg5* transcripts (Fig. 1n). As development proceeds, *plekhg5* expression in the hindbrain region is seen as two distinct domains, with the anterior chevron-shaped domain reminiscent of the rhombic lip structure that contributes to future cerebellum (Fig. 1o). In tadpoles, *plekhg5* expression remains in the hindbrain region, pharyngeal pouches, and the tip of the tails (Fig. 1p and q). In addition, ventral mesodermal cells show increasing *plekhg5* expression from tailbud stages onward (Fig. 1l, p, and q). Bisected embryos reveal notochordal and dorsal neural staining of *plekhg5* transcripts at the tail (Fig. 1r), whereas more anterior regions have transient expression of *plekhg5* in the notochord that disappears at slightly later stages (Fig. 1t to w). Neural crest cells migrating toward and in the dorsal root ganglia also contain *plekhg5* (Fig. 1t to w). Furthermore, embryos bisected along the horizontal plane show specific *plekhg5* signals at the tips of the protruding pharyngeal pouches and in the epithelial cells lining the pharyngeal cavity (Fig. 1s). The dynamic expression of *plekhg5* in tissues undergoing morphogenesis and in migrating cells suggests that this gene may regulate epithelial bending and other morphogenetic processes during early *Xenopus* development.

Ectopic expression of *plekhg5* induces blastopore lip-like morphology in a Rho-dependent manner

To examine the function of *plekhg5*, we first injected *plekhg5* RNA into the animal region of 2-cell stage embryos. Cells with concentrated pigmentation and reduced apices were observed at early blastula stages, with apical cell surface areas of darkly pigmented cells reducing to about one-third of that of their neighboring cells or cells in control embryos (Fig. 2A, Suppl. Fig. 1). When comparing with the growth factor activin which has been shown to induce ectopic bottle cells in the animal region (Kurst and Hausen, 2000), we observed that activin treatment induced ectopic blastopore lip at early gastrula, but not blastula, stages (Fig. 2A and Suppl. Movie 1). This suggested that activin might induce ectopic *plekhg5* expression when inducing ectopic blastopore lip, an idea that was supported by our ISH results (Fig. 2B). As Rho signaling has been implicated in bottle cell formation in *Xenopus* (Ossipova et al., 2015), we examined whether over-expression of *rhoA* was sufficient to induce ectopic blastopore lip. Injection of 10 fold higher doses of *rhoA* than that of *plekhg5* RNA (1ng vs. 0.1ng) did not result in ectopic bottle cells formation (Fig. 2C). In addition, *arhgef3*, another RhoGEF enriched in the early

organizer of *Xenopus* embryos (Hufton et al., 2006), did not induce ectopic blastopore lip in the animal region either (Fig. 2C). To confirm that Rho signaling is required by *plekhg5* to induce ectopic blastopore lip, we co-injected *plekhg5* with a dominant negative *rhoA* construct (DN-*rhoA*, or *rhoA*-T19N). DN-*rhoA* blocked bottle cell induction by *plekhg5*, whereas DN-*rac1* (*rac1*-T17N) was inefficient in doing so (Fig. 2D, Suppl. Fig. 2). Furthermore, neither DN-*Rab11* nor Vangl2-MO, which have been shown to regulate bottle cell formation in Xenopus (Ossipova et al., 2015), blocked *plekhg5* (Suppl. Fig. 3). Induction of the blastopore lip-like morphology by *plekhg5* was not limited to the animal region, as marginal or vegetal injection of the RNA also induced darkly pigmented cells in those regions (Fig. 2E). ISH of the mesodermal markers *brachyury* and *goosecoid* revealed that while activin-dependent ectopic bottle cell induction was associated with expression of these markers, neither gene was turned on by *plekhg5* (Suppl. Fig. 4). In addition, cells involuted through the ectopic lip induced by activin, whereas *plekhg5* caused bending of the ectodermal sheet toward the darkly pigmented cells without efficient invagination (Suppl. Movie 1). Taken together, the results demonstrate that *plekhg5* directly induces cell morphological changes in a Rho-dependent manner without invoking cell fate changes, and that the activity of *plekhg5* cannot be attributed simply to general Rho activation in a cell, but may rely on localized regulation of subcellular Rho signaling.

plekhg5 **promotes elongation of the superficial epithelial cells**

To analyze how *plekhg5* modulates cell shape, we co-injected RNAs of *plekhg5* and membrane-targeted mCherry fluorescent protein in the animal region of early embryos. Cell morphology was examined at early gastrula stages with both *en face* and side views by confocal microscopy. In control embryos, cells displayed similar sizes from the *en face* view and showed cuboidal shape from the side view (Fig. 3A). In *plekhg5*-expressing embryos, cells with dark pigmentation showed enhanced mCherry signals and a mixture of many smaller apices intermingled with several large ones, implying that overexpression of *plekhg5* might create a mechanical competition between neighboring cells, in which tension generated by apically constricting cells with reduced apical areas stretched adjacent cells with enlarged apical surfaces. Side view of the cells revealed that the outer epithelial cells had an elongated morphology, many without basal expansion, whereas the deeper cells retained the round shape (Fig. 3A). Measurement of the ratio of apical-basal cell height over apical cell width of the superficial epithelial cells showed

that in the *plekhg5*-expressing embryos, the ratio had a significant increase of 81% over that in control embryos (Fig. 3B). In addition, ectopic *plekhg5* expression prevented radial cell intercalation in the animal region so that multi-layered inner cells were observed without the ectodermal thinning seen in the control embryos (Suppl. Fig. 5). The data indicate that *plekhg5* acts differentially in epithelial and mesenchymal cells and that *plekhg5* regulates apical constriction and apical-basal cell elongation in superficial epithelial cells.

***plekhg5* stimulates apical actomyosin accumulation in outer epithelial cells**

Apical constriction is often the result of polarized localization and activation of the actomyosin contractile machinery. To examine how *plekhg5* regulates actomyosin cytoskeleton, we stained the bisected embryos or dissected animal caps with Alexa Fluor 488-conjugated phalloidin to visualize F-actin and performed fluorescence immunocytochemistry using anti-phosphorylated myosin light chain (pMLC) antibody to detect activated myosin (Fig. 3C, Suppl. Fig. 6). In control embryos, F-actin was seen mainly at the cell junctions, whereas in *plekhg5*-expressing embryos, F-actin was strongly enriched underneath the apical cell membrane in outer epithelial cells (arrows), but showed a cell contact-associated distribution in the inner cells that was similar to that in control embryos (Fig. 3C, Suppl. Fig. 6). Similarly, pMLC signal was detected mainly at the cell borders of the superficial cells, but showed an apical enrichment in *plekhg5*-expressing embryos (arrows, Fig. 3C, Suppl. Fig. 6). The data thus demonstrate that *plekhg5* facilitates polarized actomyosin accumulation in the apical cell cortex in superficial epithelial cells.

Plekhg5 is localized apically in superficial epithelial cells

The polarized enrichment of apical actomyosin cytoskeleton suggests that Plekhg5 protein may be localized in a polarized fashion in epithelial cells. To test this, we inspected Plekhg5 protein distribution using a green fluorescent protein (GFP) – tagged Plekhg5 that preserved its ability to induce ectopic blastopore lip in *Xenopus* embryos (Fig. 4). When expressed in the ectoderm, GFP-Plekhg5 was detected at high levels near the apical cell surface of the outer epithelial cells but was diffuse in cells of the deeper layers (arrows, Fig. 4A).

Plekhg5 contains a pleckstrin homology (PH) domain and a PDZ-binding motif (PBM) in addition to the GEF domain (Fig. 4B). To test the role of these domains in Plekhg5 localization,

we made two deletion mutants that removed the PH and the PBM domains, respectively. Functional studies showed that deletion of the PH domain, but not the PBM motif, rendered the mutant protein incapable of inducing an ectopic blastopore lip (Fig. 4B). Consistent with the functionality, deletion of the PBM motif did not alter the apical enrichment of the mutant protein, but deletion of the PH domain led to the loss of apical accumulation of Plekhg5 (Fig. 4C). Western blot analysis demonstrated that all the proteins were expressed at the similar levels (Suppl. Fig. 7). To see whether the GEF activity is required for apical localization of the protein, we also made a point mutation that altered the conserved threonine at the amino acid position 365 in the GEF domain to phenylalanine (T365F, Aghazdeh et al., 1998; Liu et al., 1998). This GEF mutant could not induce ectopic blastopore lip, but was recruited to the cell junctions in the superficial epithelial cells (yellow arrows, Fig. 4). However, unlike wild type Plekhg5, T365F mutant was not enriched underneath the apical cell membrane (Fig. 4C). The results establish that apical accumulation of Plekhg5 in the outer epithelial cells requires both the PH domain and the GEF activity.

plekhg5 is required for blastopore lip formation

To examine the endogenous function of *plekhg5* during blastopore lip formation, we designed two splicing-blocking (SB) antisense morpholino oligos (MOs). SB-MO1 targeted the 3' junction of exon 8 and the following intron, whereas SB-MO2 spanned the 3'-end of the exon 7 and the adjacent intron (Fig. 5A). These SB-MOs blocked the splicing donor sites that were conserved between both L and S alloalleles in *Xenopus laevis*, leading to intron retention and premature translational termination. The resulting truncated protein lacked the GEF domain and was expected to be non-functional. RT-PCR analysis of *plekhg5* RNA transcripts from the morphant embryos at gastrula stages showed that both SB-MOs worked efficiently to block RNA splicing of both L and S alloalleles (Fig. 5B, C). When injected into the marginal zone of early frog embryos, the MOs blocked formation of the blastopore lip. Depending on the site of MO injection, blastopore lip from the dorsal, lateral or ventral regions could be affected (Fig. 5D, Suppl. Fig. 8A). The inhibition of blastopore lip was not due to altered mesodermal specification, as both the prechordal marker *goosecoid* (*gsc*) and the trunk mesodermal marker *brachyury* (*bra*) were expressed in the morphant embryos, though the movements of the tissues expressing these markers were impaired (Fig. 5E). The defects in blastopore lip formation in the morphant

embryos were largely rescued when the SB-MOs were co-injected with low doses of full length *plekhg5* RNA (Fig. 5F, Suppl. Fig. 9), demonstrating that the morphant phenotype was specific to the knockdown of the *plekhg5* gene.

Knockdown of *plekhg5* prevents ectopic induction of the blastopore lip by activin

As activin induced ectopic bottle cells in the animal region with concurrent induction of *plekhg5* (Fig. 2), we addressed whether *plekhg5* was essential for activin-dependent ectopic blastopore lip formation. Indeed, we observed that upon co-expression with *plekhg5*-MO, activin could no longer induce ectopic bottle cells even though it induced mesodermal markers efficiently (Fig. 5G, Suppl. Fig. 8B). The results indicate that *plekhg5* is not required for mesodermal fate specification by activin, but its protein product is obligatory in activin-induced blastopore lip formation. Since both SB-MOs produced similar phenotypes in all our assays (Fig. 5 and Suppl. Fig. 8), we focused on SB-MO1 (referred to as SB-MO) in all our following experiments.

***plekhg5* regulates morphology and apical actomyosin enrichment in bottle cells during blastopore lip formation**

Bottle cells of *Xenopus* gastrulae assume a distinct morphology of a narrow cell apex, an elongated cell body and the expansion of the basolateral cell compartment. To see how *plekhg5* regulates bottle cell shape, we examined cell morphology with both the surface view, which revealed both isotropic shrinkage of cell areas and the fusiform-like narrowing of the cell apex in control cells, and the side view, which showed a flask-shaped cell contour of these cells (Fig. 6A). In *plekhg5* morphant embryos, the constriction of cell apices was not seen from the surface view and the cells took on a cuboidal or a columnar shape when viewed from the sagittal plane (Fig. 6A). Despite this, there were signs of gastrulation movements in the absence of bottle cell constriction (pink arrow, Fig. 6A). Phalloidin staining of the bisected embryos showed an enrichment of F-actin near the apical membrane of the bottle cells in control embryos (yellow arrows, Fig. 6B), whereas in *plekhg5* morphant embryos, apical F-actin was detected but no concentrated F-actin signal enrichment was observed (Fig. 6B). Activation of myosin, marked by pMLC signal, was seen to be enriched around the apical cell membrane in the bottle cells in control embryos, but no apical pMLC signal was detected in the *plekhg5* morphant embryos. Instead, pMLC was distributed around the basolateral membrane in the epithelial cells (Fig. 6B).

The results demonstrate that *plekhg5* facilitates apical assembly of actomyosin cytoskeleton in the bottle cells to promote efficient apical constriction during blastopore lip formation.

Gastrulation movements proceed with imprecision in the absence of the blastopore lip

As indicated by the groove formed in the *plekhg5* morphant embryos (Fig. 6A), cells might retain the ability to internalize in the absence of apical constriction of the bottle cells. To further analyze gastrulation movements in the absence of the blastopore lip, we performed time lapse video microscopy to track tissue movements in wild type and *plekhg5* morphant embryos (Fig. 6C and Suppl. Movies 2-4). Knockdown of *plekhg5* did not affect epiboly, as animal cells continued to move down and accumulated in several layers above the marginal zone (red arrowhead, Fig. 6C). Vegetal endodermal cell rotation also seemed to proceed normally, as thinning of the vegetal mass, which was more pronounced on the dorsal side, was observed (red arrow, Fig. 6C). Cell invagination and involution eventually occurred at a delayed time when the sibling embryos entered the neurula stages, and convergent extension might have provided the key driving force for blastopore formation and closure in the absence of the bottle cells (Suppl. Movies 2, 3). Although blastopore closure was seen in embryos with minimal blastopore lip at the mid-gastrula stages with the injection of the *plekhg5* SB-MO in all blastomeres of 4-cell stage embryos (Suppl. Movie 3), we did observe aberrant cell movements and failure in blastopore closure in about 20% of the embryos (Suppl. Fig. 9 and Suppl. Movie 4), implying that cell movements in the absence of the bottle cells were less precise and prone to errors. Our data thus demonstrate that several morphogenetic movements can occur in the absence of the *plekhg5*-dependent formation of the bottle cells to close the blastopore during *Xenopus* gastrulation. However, the delay in blastopore closure and the relaxation in movement precision is associated with developmental defects in the tadpoles (Suppl. Fig. 9).

Discussion

Apical constriction is an important cellular process that regulates cell shape changes during multiple developmental processes in diverse animal species. One crucial driving force in initiating and promoting apical constriction is the activation of the actomyosin contractile machinery specifically at the apical cell domain. This step is often controlled temporally and spatially to ensure that changes in individual cell morphology coordinate with global tissue

morphogenesis patterns. Different animals employ distinct strategies to regulate apical actomyosin, with most strategies converging at the level of modulating Rho family of small GTPase activity. Understanding the function of tissue-specific regulators of Rho proteins during apical constriction can thus provide insight into cellular and molecular mechanisms regulating this fundamental cell process. In this study, we report that the RhoGEF gene *plekhg5* plays an essential role in controlling apical constriction of the bottle cells during *Xenopus* gastrulation.

Expression of *plekhg5* in cells undergoing apical constriction

One major question regarding apical constriction is what factor(s) specify a particular group of cells to undertake the cell shape changes in particular embryonic regions at particular developmental stages. Studies from different animal models indicate that cell fate determination factors often regulate cell apical constriction. In *C. elegans*, transcription factors responsible for endodermal and mesodermal cell lineages are required for waves of sequential internationalization of the corresponding cells. Ectopic formation of endodermal or mesodermal cells is sufficient to induce ectopic apical constriction of these cells at the relevant times (Nance and Priess, 2002; Nance et al., 2005; Lee et al., 2006; Rohrschneider and Nance, 2009; Harrell and Goldstein, 2011). Similarly, *Drosophila* mesodermal determination transcription factors Snail and Twist control apical constriction of ventral furrow cells via their downstream targets, such as folded gastrulation (*fog*) and T48, that regulate actomyosin (Leptin and Grunewald, 1990; Martin et al., 2009; Sawyer et al., 2010; Manning and Rogers, 2014). In *Xenopus*, nodal signaling specifies mesodermal and endodermal cell fates in a dose-dependent manner, and ectopic expression of nodal family ligands in the animal region induces ectopic bottle cell formation in conjunction with mesendodermal markers. Both morphological features and cell cycle control of these ectopic bottle cells are indistinguishable from those at the endogenous positions (Kurth and Hausen, 2000; Kurth 2005). Hence *Xenopus* bottle cell formation is also linked to cell fate determination, and nodal signaling can function to connect embryonic patterning and morphogenesis. However, the fact that the bottle cells are present specifically in a narrow ring around the blastopore suggests that nodal downstream factors are likely engaged in positive and negative feedback control to precisely position the bottle cells within a narrow domain. Based on the expression pattern and the function of *plekhg5*, we speculate that nodal controls bottle cell formation via transcriptional regulation of *plekhg5*. Once *plekhg5* is turned

on, it is sufficient to induce apical constriction in all epithelial tissues regardless of cell fate. However, in cells of epidermal fate, *plekhg5*-induced apical constriction often presents without concurrent basal expansion, implying that mesendodermal fate may be important for basal protrusion and expansion in bottle cells. The specific expression of *plekhg5* may also contribute to distinct cell behaviors after internalization of mesendodermal cells in diverse amphibian species. Bottle cells form in epithelia of both endodermal and mesodermal fate in variable amounts in different species of amphibian, and their timing of undergoing apical constriction, and if and when they undergo EMT and ingression to form deep mesenchymal mesodermal cells or re-spread to form an epithelial endodermal sheet, also varies according to species (Shook et al., 2002, 2004; Shook and Keller, 2008a, b). *plekhg5* may be the key component in regulation of apical constriction across different nodal-induced tissue fates. Thus, understanding how *plekhg5* expression is controlled becomes critical in comprehending how bottle cells are positioned in gastrulating embryos. Sequence analysis of *plekhg5* promoter and putative enhancer regions reveals multiple transcription factor binding motifs, including those of Smad, Sox proteins, and T-box transcription factors. Genome-wide ChIP-seq studies indeed show that Smad2/3 and Foxh1, the transcriptional effectors of nodal signaling, can bind to the *plekhg5* enhancer directly (Chiu et al., 2014). Further detailed dissection of the functional DNA elements and their binding factors involved in *plekhg5* expression will be a promising avenue to investigate bottle cell induction at gastrulation. It is interesting to note here that transcriptional regulation that determines cells undergoing apical constriction is not limited to bottle cells at gastrulation. Shroom3, an actin binding protein that is necessary and sufficient for apical constriction of neural hinge cells during neural tube closure, also seems to be regulated at the transcriptional levels in the neural plate (Haigo et al., 2003; Hildebrand, 2005; Lee et al., 2007, 2009). It will be interesting to examine in the future whether transcriptional control of specific actomyosin regulators is a general theme to induce cell apical constriction in other contexts, such as in developing gut or during lens morphogenesis (Chung et al., 2010; Plageman et al., 2010). At later stages, dynamic *plekhg5* expression is also observed in tissues undergoing epithelial morphogenesis, such as the forming otic vesicles and the tip of the protruding pharyngeal pouches. Plekhg5 may thus regulate additional apical constriction events during organogenesis. In addition, expression of *plekhg5* in discrete migratory and mesenchymal cell populations

suggests that it may play roles in controlling cell morphology and directional movements during late embryogenesis.

Apical localization of the Plekhg5 protein

Apical actomyosin activation is a common theme for cell shape changes in gastrulating embryos, but different animals use distinct mechanisms to achieve this effect. In *Drosophila*, two Twist target genes, the transmembrane protein T48 and the secreted factor *fog*, regulate apical localization of the PDZ-domain-containing DRhoGEF2 in a partially redundant fashion (Kolsch et al., 2007). The Twist-T48-fog pathway does not affect DRhoGEF2 associated with cell junctions, but is required for medioapical accumulation of DRhoGEF2 to regulate apical actomyosin dynamics through the Rho1/RhoA and Rok/ROCK signaling pathway during ventral furrow formation (Sawyer et al., 2010, Manning and Rogers, 2014; Mason et al. 2016). In *C. elegans*, apical activation of actomyosin relies on polarized localization of a Cdc42 GAP protein PAC-1 via cell-cell contact-mediated recruitment of PAC-1 to the basolateral domain, leaving active Cdc42 at the contact-free apical surface to stimulate MRCK-1 activity (Lee and Goldstein, 2003; Anderson et al., 2008; Chan and Nance, 2013; Marston et al., 2016). Our studies reveal a similarity to *Drosophila* development in that *Xenopus* also utilizes an apically localized RhoGEF, Plekhg5, to organize a polarized actomyosin cytoskeleton at the cell apex. However, unlike fly DRhoGEF2, Plekhg5 does not contain a PDZ domain, and no vertebrate T48 or Fog homologs exist. Apical recruitment of Plekhg5 thus relies on a different mechanism. Plekhg5 contains both PH and PBM domains in addition to the GEF motif, and the PBM domain of Plekhg5 homologs has been shown to bind the multiple PDZ-domain-containing factor MUPP1 and its family member Patj in mammalian cells, zebrafish and *C. elegans* (Estevez et al., 2008; Ernkvist et al., 2009; Lin et al., 2012). Since Patj is an apically localized tight junction protein in the Crumbs protein complex (Tepass 2012), it is conceivable that Plekhg5 is recruited to the apical surface via its interaction with Patj. However, our structure-function analysis reveals that the PBM domain is dispensable for Plekhg5 localization and function, suggesting that other factors are involved in recruiting Plekhg5. Removal of the PH domain abolishes Plekhg5 apical positioning, indicating a crucial role of the PH motif in Plekhg5 localization. As PH domains can interact with phospholipids in addition to other proteins (Krahn and Wodarz, 2012), it is possible that binding to the apical membrane lipid phosphotidylinositide 4,5 phosphate helps to

recruit Plekhg5 to the apical compartment. This ability is not shared among all PH-containing RhoGEFs, as another organizer-enriched RhoGEF, Arhgef3, localizes mainly in cell nucleus and cannot induce apical constriction when ectopically expressed (Fig. 2, Suppl. Fig. 10). The PH domain has also been shown to regulate GEF activities independently of its membrane association (Bi et al., 2001; Baumeister et al., 2006). As the GEF mutant protein can localize to the apical junction but is not enriched in apical cell cortex (Fig. 4), it is possible that compromise of the GEF function contributes to the loss of apical enrichment of Plekhg5 in both PH deletion and T365F mutants. Taken together, our data suggest the model that Plekhg5 is recruited to the cell junction independently of PBM or the GEF activity, but its enrichment at the apical cortex requires the PH domain and the intact GEF function. Further investigation is needed to test this model and identify the protein(s) and/or the lipid components that interact with Plekhg5 directly.

Rho and its downstream signaling in apical constriction

Localized activation of Rho GTPases controls polarized distribution and activation of actomyosin during apical constriction. Depending on the member of the Rho family GTPases activated, different effectors are involved to control actomyosin activity. For example, MRCK (myotonic dystrophy kinase-related Cdc42-binding kinase) is activated downstream of Cdc42 in *C. elegans* to phosphorylate myosin regulatory light chain and induce cytoskeleton contraction to drive apical constriction (Anderson et al., 2008; Marston et al., 2016). In *Drosophila*, Rho1/RhoA signaling acts downstream of DRhoGEF2 to control activities of Rho-dependent protein kinase (ROCK) and Diaphanous (Dia) during cell invagination (Barrett et al., 1997; Hacker and Perrimon, 1998; Mason et al., 2013). Our experiments show that blocking RhoA but not Rac1 prevents blastopore lip induction (Fig. 2), a result consistent with *plekhg5* being a Rho-specific GEF (Marx et al., 2005). Though it is conceivable that ROCK and Dia act downstream of *plekhg5*/*rhoA* to regulate actomyosin in *Xenopus*, application of the ROCK inhibitor Y-27632 is ineffective in blocking blastopore lip formation (Lee and Harland, 2007; Suppl. Fig. 11). It is unclear whether this is due to insuffficient penetration of the inhibitor into the cells or it is because of the employment of other downstream effectors, such as Citron kinase (Thumkeo et al., 2013), in bottle cell formation. Further investigation of the roles of ROCK, Dia, and Citron kinase will be informative to identify *plekhg5*/*rhoA* effectors that mediate their function on actomyosin contraction and apical constriction in *Xenopus*.

Gastrulation movements in the absence of the bottle cells

Though the appearance of the bottle cells is a striking external indication of gastrulation movements in *Xenopus*, bottle cells per se do not seem to be absolutely required. Both surgical removal of these cells (Hardin and Keller, 1988) and the prevention of bottle cell formation in *plekhg5* morphant embryos can result in complete, albeit delayed, blastopore closure. In the absence of the bottle cells, vegetal rotation - the amoeboid migration movements of the yolky endodermal and mesendodermal cells upward and laterally against the blastocoel walls (Winklbauer and Schurfeld, 1999; Wen and Winklbauer, 2017) - proceeds normally, so that a clear area of cells, reflecting thinning of the endoderm, often forms on the dorsal vegetal side. Epiboly movements of the animal cells also occur normally as in the control embryos. Mesodermal cell involution seems to be delayed and may happen at more variable positions in the marginal zone, so that the *goosecoid*-expressing domain is positioned at variable distances from the blastopore at late gastrulation (Fig. 5, 6). The eventual blastopore closure appears to be driven mainly by convergent extension movements during neurulation, as body elongation helps to push the surface tissues toward the blastopore to facilitate mesendodermal internalization. Blastopore closure seems to proceed with somewhat variable speeds among morphant embryos, with a small portion failing, especially those expressing the SB-MO2 (Suppl. Fig. 9). The data suggest that although formation of the blastopore lip is not obligatory for gastrulation movements, it may facilitate coordination of different cell movements and ensure the robustness and reproducibility of gastrulation. The compensation for lack of apical constriction during gastrulation has also been observed in other animals (Llimargas and Casanova, 2010). In sea urchin, laser ablation of the bottle cells surrounding the vegetal plate delays but does not abolish the invagination of the vegetal plate (Nakajima and Burke, 1996; Kimberly and Hardin, 1998). In *C. elegans*, endodermal cells partially internalize into the embryos in the absence of an apical actomyosin network (Nance et al., 2003). It is thus apparent that multiple mechanisms are involved in gastrulation morphogenesis and they work in partially redundant manner to enable the correct placement of endodermal and mesodermal cells inside the embryos. Apical constriction-mediated cell shape changes help to orchestrate a robust cell movement program for reproducible embryonic patterning and development.

plekhg5 in other tissue contexts

Apical constriction is used reiteratively in multiple developmental contexts. One well studied process is neural tube closure, with the apical constriction of hingepoint cells in the neural plate as a crucial step (Suzuki et al., 2012; Wallingford et al., 2013). In situ hybridization of *plekhg5* does not reveal prominent signal in the hingepoint cells, and *plekhg5* morphant embryos do not show obvious neural tube closure defects. This indicates that *plekhg5* may not participate in neural tube closure. Instead, another RhoGEF, GEF-H1/*arhgef2*, has been shown to regulate apical constriction of neural cells in *Xenopus* (Itoh et al., 2014). Multiple other factors also participate in control of apical constriction of hingepoint cells in *Xenopus* neural plate (review in Suzuki et al., 2012). Although *plekhg5* is not involved in neural tube closure, its expression in several other places, such as the otic vesicle and the cells at the turning points of the protruding pharyngeal pouches, imply that it may regulate apical constriction during organogenesis. In mammalian cell culture and in zebrafish, *plekhg5* homologs are also shown to regulate directional migration of cancer and endothelial cells and vasculature formation (Liu and Horowitz, 2006; Garnaas et al., 2008; Ernkvist et al., 2009; Dachsel et al., 2013). This suggests that in migrating cells, *plekhg5* may interact with other partners for localized activation of Rho and actomyosin to provide positional cue for directional movement. Further studies will reveal how *plekhg5* controls context-dependent polarization of actomyosin to influence different cell behaviors.

Materials and methods

Obtaining embryos and microinjection

Xenopus laevis frogs were used throughout the study (under the institutional IACUC protocol 09658). Female frogs were primed with 800 units/frog of human chorionic gonadotropin hormone (Sigma) the night before usage. Embryos were obtained by in vitro fertilization, dejellied with 2% cysteine solution, and micro-injected with RNAs or antisense MOs. The animal regions of both blastomeres of 2–cell stage embryos or the marginal zone regions of the two dorsal or two ventral cells of 4-cell stage embryos were injected, as indicated in the text. For vegetal injection, *plekhg5* RNA was injected into one vegetal blastomere at stages 6 to 7 to circumvent transportation of the injected RNA into the marginal area by cytoplasmic streaming (Danilchik and Denegre, 1991).

Plasmids and antisense morpholino oligonucleotides (MOs)

The *plekhg5* coding sequence was PCR-amplified from gastrula stage cDNA, with the N- and the C-terminal primer sequences: Plekhg5-N(NotI): 5’-AGAAGCGGCCGCACCATGGTATGTCA

TCATGCAGACTG-3' and Plekhg5-C(XhoI): 5'-CCGCTCGAG TTACACCTCTGAAGCC GTTAATGTAG-3'. The coding sequence was inserted between the NotI and XhoI sites of the pCS105 vector. GFP-tagged *plekhg5* was constructed by inserting the ligation product of NheI/SalI fragment of pEGFP-C3 and SalI/AscI fragment of *plekhg5* into the XbaI/AscI sites of the pCS105 vector. The *plekhg5* mutants were made using a PCR-based method with the primers: plekhg5-PH-del-for: CACACACAATTGGCACAGAATCTCTTGCAAAGAACGAG; plekhg5-PH-del-rev: TGTGTGCAATTGTGTATCTTCAGGAGATGTTCCAATC; plekhg5-DPBM-C(XhoI): CCGCTCGAGTTATGAAGCCGTTAATGTAGAGTT. All the plasmids were linearized with the AscI enzyme before being transcribed with the SP6 RNA polymerase. 100-200pg of *plekhg5* or its mutant RNAs were used for injection. The sequences of *plekhg5* splicing-blocking MOs are: SB-MO1: 5'-ACAAATTACCTCAGGAACCTCAATG-3' and SB-MO2: 5'-AGGCAAATATCTTACCCTTCCAAA-3', both targeting the exon-intron junctional sequences for intron retention. 20-50ng MOs were injected in the experiments.

RT-PCR

To assay for the efficiency of *plekhg5* splicing-blocking MOs, several primer pairs were designed. The sequences of the primers 1 to 6 (Fig. 5A) are: primer 1 (exon 8, forward): 5'-CAAGTTGCATTCATACAGTATGTTTG-3'; primer 2 (exon 10, reverse): 5'-TCCGGACTCTTGTAGATTCAACAG-3'; primer 3 (intron 8 of *plekhg5*.L, forward): 5'-GAACAGATTTAGGATTGATAGGTCAG-3'; primer 4 (intron 8 of *plekhg5*.S, forward): 5'-GAACAtATTTAGAATTGATAAGTCAG-3'; primer 5 (exon 7, forward): 5'-GACGCAAGTATTCCGGTACAAGATC-3'; primer 6 (intron 7, reverse): 5'-GGCAATTTTAGCAGTTTGTATAGAAA-3'. The expected sizes of the PCR products are: primers 1+2 (no intron): 277bp; primers 3+2 (*plekhg5*.L intron retention with SB-MO1): 508bp; primers 4+2 (*plekhg5*.S intron retention with SB-MO1): 385bp; primers 5+2 (no intron): 441/447bp (L/S alloalleles); primers 5+6 (intron retention with SB-MO2): ~270bp (S alloallele is not annotated clearly).

In situ hybridization (ISH)

ISH was performed as described by Harland (1991). For *plekhg5* in situ, the C-terminal fragment of the coding sequence was used as the probe. The embryos were bisected before or after staining to reveal internal signals.

F-actin staining and Immunofluorescence (IF)

For F-actin staining, embryos or explants were fixed in MEMFA for 30 minutes, washed with PBS three times, and stained with 5 units/ml Alexa Fluor 488-conjugated phalloidin (Invitrogen) in PBS with 0.1% Tween 20 for 3 hours at the room temperature or overnight at 4°C. For immunocytochemistry of phosphorylated myosin light chain, we adopted the protocol described in Lee and Harland (2007). Anti-phospho-Ser20 myosin light chain rabbit antibody (Abcam ab2480, 1:500) and Alexa Fluor 488-conjugated secondary antibody (Life Technologies A-11070, 1:200) were used.

Imaging

For stereo imaging of embryonic phenotypes and in situ hybridization, Zeiss M2Bio and Nikon AZ100 microscopes were used. For time-lapse movies, embryos were positioned to the correct orientations (animal or vegetal side up) using modeling clay, and 6 to 8 hour time-lapse imaging was performed with 3-minute intervals. For fluorescence microscopy, Olympus Fluoview 2000 upright confocal microscope was used. Some of the embryos were bisected across the dorsal-ventral midline before imaging. Most of the images were taken using a 20X (NA0.95) lens. Maximum projections of Z-stack images were used for the figures.

Morphometric and statistical analysis

The surface areas of blastula stage embryos and the height-to-width (H/W) ratio of the outer epithelial animal cells were measured using NIH ImageJ software. For apical cell areas at the blastula stages, a total of 362 cells from 31 control embryos, 347 darkly pigmented cells from 32 *plekhg5*-injected embryos, and 350 normal pigmented cells from 32 *plekhg5*-injected embryos from 4 independent experiments were examined. For H/W ratio, a total of 153 cells from 28 control embryos and 129 cells from 26 *plekhg5*-injected embryos from 3 independent experiments were measured. Scatter plot of individual dataset was performed using GraphPad Prism7 software. The student t-test was used to assess the statistical significance in differences between control and *plekhg5*-injected samples.

Acknowledgements

We are grateful to Dr. Jianbo Wang for allowing us to use his Olympus Fluoview confocal microscope.

Competing Interests

None.

Funding

The study is supported by NIH grants R01GM098566 to CC and RK and R01GM099108 to PS.

References

Aghazadeh, B., Zhu, K., Kubiseski, T.J., Liu, G.A., Pawson, T., Zheng, Y. and Rosen, M.K. (1998) Structure and mutagenesis of the Dbl homology domain. Nature Struct. Biol. 5, 1098-1107.

Anderson, D.C., Gill, J.S., Cinalli, R.M. and Nance, J. (2008) Polarization of the C elegans embryo by RhoGAP-mediated exclusion of PAR-6 from cell contacts. Sci. 320, 1771-1774.

Barmich, M.J., Rogers, S. and Hacker, U. (2005) DRhoGEF2 regulates actin organization and contractility in the Drosophila blastoderm embryo. J. Cell Biol. 168, 575-585.

Barrett, K., Leptin, M. and Settleman, J. (1997) The Rho GTPase and a putative RhoGEF mediate a signaling pathway for the cell shape changes in Drosophila gastrulation. Cell 91, 905-915.

Baumeister, M.A., Rossman, K.L., Sondek, J. and Lemmon, M.A. (2006) The Dbs PH domain contributes independently to membrane targeting and regulation of guanine nucleotide-exchange activity. Biochem J. 400, 563-572.

Beane, W.S., Gross, J.M. and McClay, D.R. (2006) RhoA regulates initiation of invagination, but not convergent extension, during sea urchin gastrulation. Dev. Biol. 292, 213-225.

Bi, F., Debreceni, B., Zhu, K., Salani, B., Eva, A. and Zheng, Y. (2001) Antoinhibition mechanism of proto-Dbl. Mol. Cell. Biol. 21, 1463-1474.

Chan, E. and Nance, J. (2013) Mechanisms of CDC-42 activation during contact-induced cell polarization. J. Cell Sci. 126, 1692-1702.

Chiu, W.T., Le, R.C., Blitz, I.L., Fish, M.B., Li, Y., Biesinger, J., Xie, X. and Cho, K.W.Y. (2014) Genome-wide view of TGFβ/Foxh1 regulation of the early mesendoderm program. Development 141, 4537-4547.

Choi, S.C. and Sokol, S.Y. (2009) The involvement of lethal giant larvae and Wnt signaling in bottle cell formation in Xenopus embryos. Dev. Biol. 336, 68-75.

Christodoulou, N. and Skourides, P.A. (2015) Cell-autonomous Ca2+ flaskes elicit pulsed contractions of an apical actin network to drive apical constriction during neural tube closure. Cell Rep. 13, 2189-2202.

Chu, C.W., Gerstenzang, E., Ossipova, O. and Sokol, S.Y. (2013) Lulu regulates Shroom-induced apical constriction during neural tube closure. PLoS ONE 8, e81854.

Chung, M.I., Nascone-Yoder, N.M., Grover, S.A., Drysdale, T.A. and Wallingford, J.B. (2010) Direct activation of Shroom3 transcription by Pitx proteins drives epithelial morphogenesis in the developing gut. Development 137, 1339-1349.

Dachsel, J.C., Ngok, S.P., Lewis-Tuffin, L.J., Kourtidis, A., Geyer, R., Johnson, L., Feathers, R. and Anastasiadis, P. (2013) The Rho guanine nucleotide exchange factor Syx regulates the balance of Dia and ROCK activities to promote polarized-cancer-cell migration. Mol. Cell. Biol. 33, 4909-4918.

Danilchik, M.V. and Denegre, J.M. (1991) Deep cytoplasmic rearrangements during early development in Xenopus laevis. Development 111, 845-856.

Das, D., Zalewski, J.K., Mohan, S., Plageman, T.F., VanDemark, A.P. and Hildebrand, J.D. (2014) The interaction between Shroom3 and Rho-kinase is required for neural tube morphogenesis in mice. Biol. Open 3, 850-860.

Ebrahim, S., Fujita, T., Millis, B.A., Kozin, E., Ma, X., Kawamoto, S., Baird, M.A., Davidson, M., Yonemura, S., Hisa, Y., Conti, M.A., Adelstein, R.S., Sagaguchi, H. and Kachar, B. (2012) NMII forms a contractile transcellular sarcomeric network to regulate apical cell junctions and tissue geometry. Curr. Biol. 23, 731-736.

Ernkvist, M., Persson, N.L., Audebert, S., Lecine, P., Sinha, I., Liu, M., Schlueter, M., Horowitz, A., Aase, K., Weide, T., Borg, J.P., Majumdar, A. and Holmgren, L. (2009) The Amot/Patj/Syx signaling complex spatially controls RhoA GFPase activity in migrating endothelial cells. Blood 113, 244-253.

Estevez, M.A., Henderson, J.A., Ahn, D., Zhu, X.R., Poschmann, G., Lubbert, H., Marx, R. and Baraban, J.M. (2008) The neuronal RhoA GEF, Tech, interacts with the synaptic multi-PDZ-domain-containing protein, MUPP1. J. Neurochem. 106, 1287-1297.

Garnaas, M.K., Moodie, K.L., Liu, M., Samant, G.V., Li, K., Marx, R., Baraban, J.M., Horowitz, A. and Ramchandran, R. (2008) Syx, a RhoA guanine exchange factor, is essential for angiogenesis in vivo. Circ. Res. 103, 710-716.

Goldstein, B. and Macara, I.G. (2007) The PAR proteins: fundamental players in animal cell polarization. Dev. Cell 13, 609-622.

Hacker, U. and Perrimon, N. (1998) DRhoGEF2 encodes a member of the Dbl family of oncogenes and controls cell shape changes during gastrulation in Drosophila. Genes Dev. 12, 274-284.

Haigo, S.L., Hildebrand, J.D., Harland, R.M. and Wallingford, J.B. (2003) Shrrom induces apical constriction and is required for hingepoint formation during neural tube closure. Curr. Biol. 13, 2125-2137.

Hall, A. (1998) Rho GTPases and the actin cytoskeleton. Science 279, 509-514.

Hardin, J. and Keller, R. (1988) The behaviour and function of bottle cells during gastrulation of Xenopus laevis. Development 103, 211-230.

Harland, R.M. (1991) In situ hybridization: an improved whole-mount method for Xenopus embryos. Meth. Cell Biol. 36, 685-695.

Harrell, J.R. and Goldstein, B. (2011) Internalization of multiple cells during C. elegans gastrulation depends on common cytoskeletal mechanisms but different cell polarity and cell fate regulators. Dev. Biol. 350, 1-12.

Hildebrand, J.D. (2005) Shroom regulates epithelial cell shape via the apical positioning of an actomyosin network. J. Cell Sci. 118, 5191-5203.

Hodge, R.G. and Ridley, A.J. (2016) Regulation of Rho GTPases and their regulators. Nat. Rev. Mol. Cell Biol. 17, 496-510.

Hufton, A.L., Vinayagam, A., Suhai, S. and Baker, J.C. (2006) Genomic analysis of Xenopus organizer function. BMC Dev. Biol. 6: 27

Itoh, K., Ossipova, O. and Sokol, S.Y. (2014) GEF-H1 functions in apical constriction and cell intercalations and is essential for vertebrate neural tube closure. J. Cell Sci. 127, 2542-2553.

Ji, Y.J., Hwang, Y.S., Mood, K., Cho, H.J., Lee, H.S., Winterbottom, E., Cousin, H. and Daar, I.O. (2014) EphrinB2 affects apical constriction in Xenopus embryos and is regulated by ADAM10 and flotillin-1. Nat. Commu. 5, 3516.

Keller, R.E. (1981) An experimental analysis of the role of bottle cells and the deep marginal zone in gastrulation of Xenopus laevis. J. Exp. Zool. 216, 81-101.

Kimberly, E.L. and Hardin, J. (1998) Bottle cells are required for the initiation of primary invagination in the sea urchin embryo. Dev. Biol. 204, 235-250.

Kolsch, V., Seher, T., Fernandez-Ballester, G.J., Serrano, L. and Leptin, M. (2007) Control of Drosophila gastrulation by apical localization of adherens junctions and RhoGEF2. Sci. 315, 384-386.

Krahn, M.P. and Wpdarz, A. (2012) Phosphoinositide lipids and cell polarity: linking the plasma membrane to the cytocortex. Essays Biochem. 53, 15-27.

Kurth, T. and Hausen, P. (2000) Bottle cell formation in relation to mesodermal patterning in the Xenopus embryo. Mech. Dev. 97, 117-131.

Kurth, T. (2005) A cell cycle arrest is necessary for bottle cell formation in the early Xenopus gastrula: integrating cell shape change, local mitotic control and mesodermal patterning. Mech. Dev. 122, 1251-1265.

Lee, C., Le, M.P. and Wallingford, J.B. (2009) The Shroom family proteins play broad roles in the morphogenesis of thickened epithelial sheets. Dev. Dyn. 238, 1480-1491.

Lee, C., Scherr, H.M. and Wallingford, J.B. (2007) Shroom family proteins regulate γ-tubulin distribution and microtubule architecture during epithelial cell shape change. Development 134, 1431-1441.

Lee, J.Y. and Goldstein, B. (2003) Mechanisms of cell positioning during C. elegans gastrulation. Development 130, 307-320.

Lee, J.Y., Marston, D.J., Walston, T., Hardin, J., Halberstadt, A. and Goldstein, B. (2006) Wnt/Frizzled signaling controls C. elegans gastrulation by activating actomyosin contractility. Curr. Biol. 16, 1986-1997.

Lee, J.Y. and Harland, R.M. (2007) Actomyosin contractility and microtubules drive apical constriction in Xenopus bottle cells. Dev. Biol. 311, 40-52.

Lee, J.Y. and Harland, R.M. (2010) Endocytosis is required for efficient apical constriction during Xenopus gastrulation. Curr. Biol. 20, 253-258.

Leptin, M. and Grunewald, B. (1990) Cell shape changes during gastrulation in Drosophila. Development 110, 73-84.

Lin, L., Tran, T., Hu, S., Cramer, T., Komuniecki, R. and Steven, R.M. (2012) RGEF-2 is an essential Rho-1 specific RhoGEF that binds to the multi-PDZ domain scaffold protein MPZ-1 in Caenorhabditis elegans. PLoS ONE 7: e31499.

Liu, M. and Horowitz, A. (2006) A PDZ-binding motif as a critical determinant of Rho guanine exchange factor function and cell phenotype. Mol. Biol. Cell 17, 1880-1887.

Liu, X., Wang, H., Eberstadt, M., Schnuchel, A., Olejniczak, E.T., Meadows, R.P., Schkeryantz, J.M., Janowick, D.A., Harlan, J.E., Harris, E.A.S. Staunton, D.E. and Fesik, S.W. (1998) NMR

structure and mutagenesis of the N-terminal Dbl homology domain of the nucleotide exchange factor Trio. Cell 95, 269-277.

Llimargas, M. and Casanova, J. (2010) Apical constriction and invagination: a very self-reliant couple. Dev. Biol. 344, 4-6.

Manning, A.J. and Rogers, S.L. (2014) The Fog signaling pathways: insights into signaling in morphogenesis. Dev. Biol. 394, 6-14.

Marston, D.J., Higgins, C.D., Peters, K.A., Cupp, T.D., Dickinson, D.J., Pani, A.M., Moore, R.P., Cox, A.H., Keihart, D.P. and Goldstein, B. (2016) MRCK-1 drives apical constriction in C. elegans by linking developmental patterning to force generation. Curr. Biol. 26, 2079-2089.

Martin, A.C., Kaschube, M. and Wieschaus, E.F. (2009) Pulsed contractions of an actin-myosin network drive apical constriction. Nature 457, 495-499.

Martin, A.C. and Goldstein, B. (2014) Apical constriction: themes and variations on a cellular mechanism driving morphogenesis. Development 141, 1987-1998.

Marx, R., Henderson, J., Wang, J. and Baraban, J.M. (2005) Tech: a RhoA GEF selectively expressed in hippocampal and cortical neurons. J. Neurochem. 92, 850-858.

Mason, F.M., Tworoger, M. and Martin, A.C. (2013) Apical domain polarization localizes actin-myosin activity to drive ratchet-like apical constriction. Nat. Cell Biol. 15, 926-936.

Mason, F.M., Xie, S., Vasquez, C.G., Tworoger, M. and Martin, A.C. (2016) RhoA GTPase inhibition organizes contraction during epithelial morphogenesis. J. Cell Biol. 214, 603-617.

McGreevy, E.M., Vijayraghavan, D., Davidson, L.A. and Hildebrand, J.D. (2015) Shroom3 functions downstream of planar cell polarity to regulate myosin II distribution and cellular organization during neural tube closure. Biol. Open 4, 186-196.

Nakajima, Y. and Burke, R.D. (1996) The initial phase of gastrulation in sea urchins is accompanied by the formation of bottle cells. Dev. Biol. 179, 436-446.

Nance, J. and Priess, J.R. (2002) Cell polarity and gastrulation in C. elegans. Development 129, 387-397.

Nance, J., Munro, E.M., and Priess, J.R. (2003) C. elegans PAR-3 and PAR-6 are required for apicobasal asymmetries associated with cell adhesion and gastrulation. Development 130, 5339-5350.

Nance, J., Lee, J.Y. and Goldstain, B. (2005) Gastrulation in C. Elegans. Wormbook, ed. The C. elegans Research Community, Wormbook, doi/10.1895/wormbook.1.23.1

Nikolaidou, K. and Barrett, K. (2004) A Rho GTPase signaling pathway is used reiteratively in epithelial folding and potentially selects the outcome of Rho activin. Curr. Biol. 14, 1822-1826.

Ohno, S. (2001) Intercellular junctions nad cellular polarity: the PAR-aPKC complex, a conserved core cassette playing fundamental roles in cell polarity. Curr. Opin. Cell Biol. 13, 641-648.

Ossipova, O., Kim, K., Lake, B.B., Itoh, K., Ioannou, A. and Sokol, S.Y. (2014) Role of Rab11 in planar cell polarity and apical constriction during vertebrate neural tube closure. Nat. Commu. 5, 3734.

Ossipova, O., Chuykin, I., Chu, C.W. and Sokol, S.Y. (2015) Vangl2 cooperates with Rab11 and Myosin V to regulate apical constriction during vertebrate gastrulation. Development 142, 99-107.

Plageman, T.F. Jr., Chung, M.I., Lou, M., Smith, A.N., Hildebrand, J.D., Wallingford, J.B. and Lang, R.A. (2010) Pax6-dependent Shroom3 expression regulates apical constriction during lens placode invagination. Development 137, 405-415.

Popov, I.K., Kwon, T., Crossman, D.K., Crowley, M.R., Wallingford, J.B. and Chang, C. (2017) Identification of new regulators of embryonic patterning and morphogenesis in Xenopus gastrulae by RNA sequencing. Dev. Biol. 426, 429-441.

Roffers-Agarwal, J., Xanthos, J.B., Kragtorp, K.A. and Miller, J.R. (2008) Enabled (Xena) regulates neural plate morphogenesis, apical constriction, and cellular adhesion required for neural tube closure in Xenopus. Dev. Biol. 314, 393-403.

Rohrschneider, M.R. and Nance, J. (2009) Polarity and cell fate specification in the control of Caenorhabditis elegans gastrulation. Dev. Dyn. 238, 789-796.

Sawyer, J.M., Harrell, J.R., Shemer, G., Sullivan-Brown, J., Rho-Johnson, M. and Goldstein, B. (2010) Apical constriction: a cell shape change that can drive morphogenesis. Dev. Biol. 341, 5-19.

Sherrard, K., Robin, F., Lemaire, P. and Munro, E. (2010) Sequential activation of apical and basolateral contractility drives ascidian endoderm invagination. Curr. Biol. 20, 1499-1510.

Shook, D.R., Majer, C. and Keller, R. (2002) Urodeles remove mesoderm from the superficial layer by sybduction through a bilateral primitive streak. Dev. Biol. 248, 220-239.

Shook, D.R., Majer, C. and Keller, R. (2004) Pattern and morphogenesis of presumptive superficial mesoderm in two closely related species, Xenopus laevis, and Xenopus tropicalis. Dev. Biol. 270, 163-185.

Shook, D.R. and Keler, R. (2008a) Epithelial type, ingression, blastopore architecture and the evolution of chordate mesoderm morphogenesis. J. Exp. Zool. (Mol. Dev. Evol.) 310B, 85-110.

Shook, D.R. and Keller, R. (2008b) Morphogenic machines evolve more rapidly than the signals that pattern them: lessons from amphibians. J. Exp. Zool. (Mol. Dev. Evol.) 310B, 111-135.

Suzuki, M., Morita, H. and Ueno, N. (2012) Molecular mechanisms of cell shape changes that contribute to vertebrate neural tube closure. Develop. Growth Differ. 54, 266-276.

Tepass, U. (2012) The apical polarity protein network in Drosophila epithelial cells: regulation of polarity, junctions, morphogenesis, cell growth, and survival. Annu. Rev. Cell Dev. Biol. 28, 655-685.

Wallingford, J.B., Niswander, L.A., Shaw, G.M. and Finnell, R.H. (2013) The continuing challenge of understanding, preventing, and treating neural tube defects. Science 339, 1222002.

Wen, J.W.H. and Winklbauer, R. (2017) Ingression-type cell migration drives vegetal endodermal internalisation in the Xenopus gastrula. eLife 6, e27190.

Winklbauer, R. and Schurfeld, M. (1999) Vegetal rotation, a new gastrulation movement involved in the internalization of the mesoderm and endoderm in Xenopus. Development 126, 3703-3713.

Figures

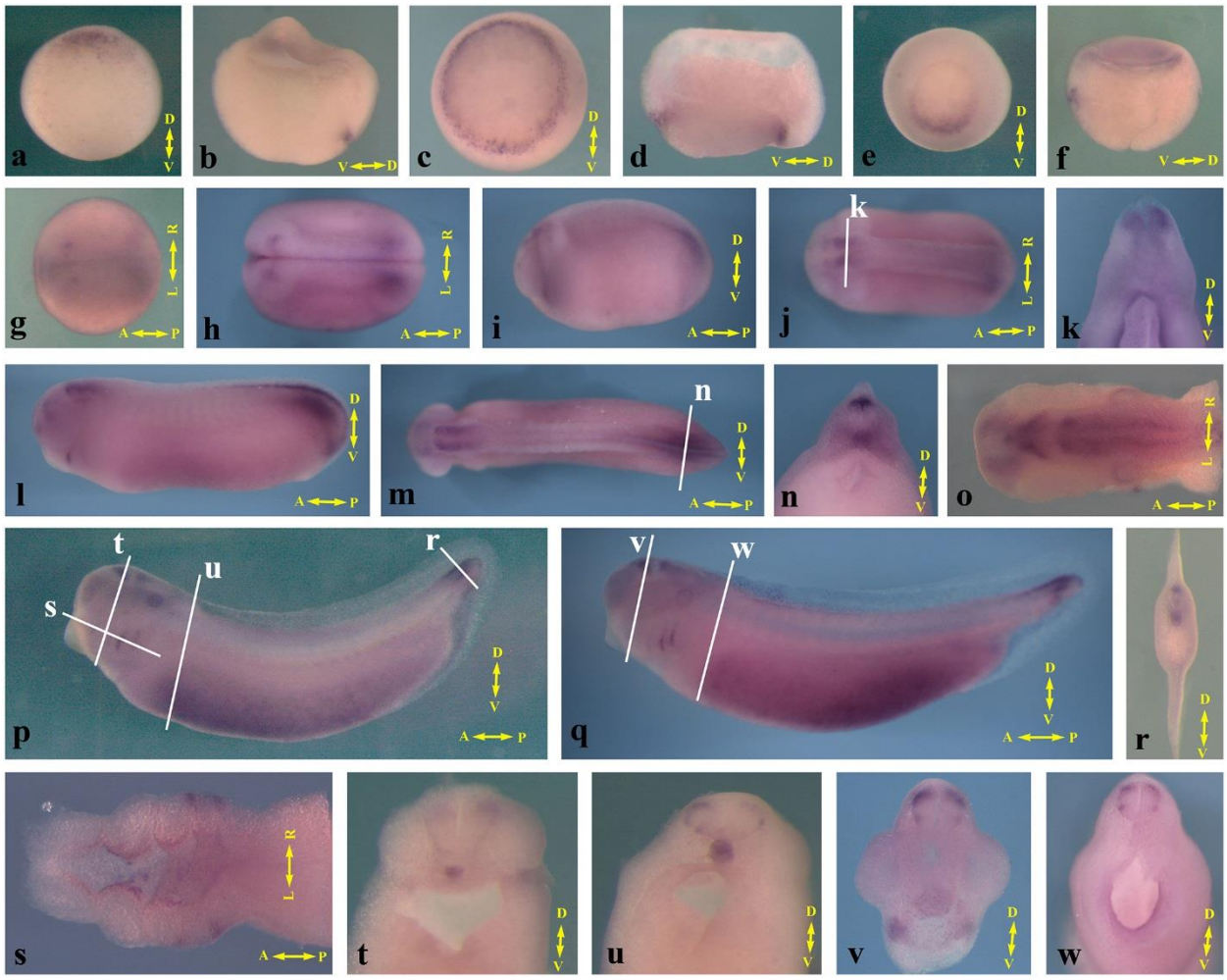

Figure 1. Dynamic expression of *plekhg5* in early *Xenopus* embryos. a-f) *plekhg5* is expressed in the blastopore lip during gastrulation. Vegetal view (panels a, c, e) and side view of bisected embryos (panels b, d, f) are shown. g-o) During neurula (panels g and h) and tailbud (panels i to o) stages, *plekhg5* is expressed in the tail, hindbrain, otic and olfactory placodes, and pharyngeal pouch. Sections of the embryos reveal *plekhg5* transcripts in the dorsal neural tube and the notochord. p and q) Expression of *plekhg5* at the tadpole stages is detected in the hindbrain, otic vesicles, tail, pharyngeal pouch, and the ventral-lateral mesoderm. r to w) Sections of the tadpole embryos show expression of *plekhg5* in the notochord - transiently in the trunk but persisting in the tail, the migrating neural crest cells along the ventral route and in the dorsal root ganglia, the dorsal neural tube in the tail, the tips of the outgrowing pharyngeal pouches, and lining of foregut. The embryonic axes are labeled in each panel: D-V, dorsal-ventral; A-P, anterior-posterior, L-R, left-right.

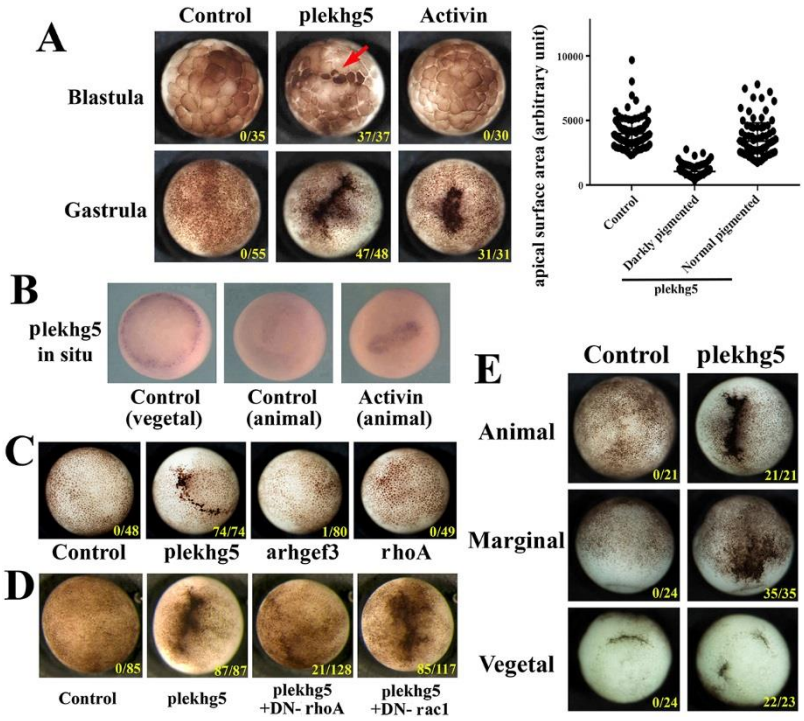

Figure 2. *plekhg5* induces ectopic blastopore lip-like morphology in early *Xenopus* embryos in a rho-dependent manner. A) *plekhg5* induces apical cell constriction in ectodermal cells at early blastula stages, whereas activin induces ectopic blastopore lip at the gastrula stages. The apical surface areas of cells at the blastula stages in control and the *plekhg5*-expressing embryos are measured and compared. Scatter plot is shown for a typical experiment. Student t-test shows that *plekhg5* significantly reduces apical cell surfaces to about 1/3 of that in control cells, with the average surface areas of 3978 and 1050 (arbitrary units) for control and apically constricted cells, respectively, and the p-value of 3.5E-31 in the experiment shown in this panel. B) Activin induces expression of *plekhg5* in the ectoderm when it induces ectopic blastopore lip. C) Unlike *plekhg5*, neither *arhgef3*, another organizer-enriched RhoGEF, nor general expression of *rhoA* induces ectopic blastopore lip morphology in the ectoderm. D) Dominant-negative *rhoA*, but not that of *rac1*, blocks ectopic blastopore lip induction by *plekhg5*. E) *plekhg5* induces ectopic blastopore lip morphology when injected either in the animal, the marginal zone, or the vegetal regions. The doses of RNAs used are 100pg of *plekhg5*, 5pg of activin, 200pg *arhgef3*, 0.5-1ng of *rhoA*, DN-*rhoA* and DN-*rac1*. The numbers of the embryos with the ectopic blastopore lip-like morphology over the total number of the embryos are shown in the panels. All the experiments are repeated at least three times.

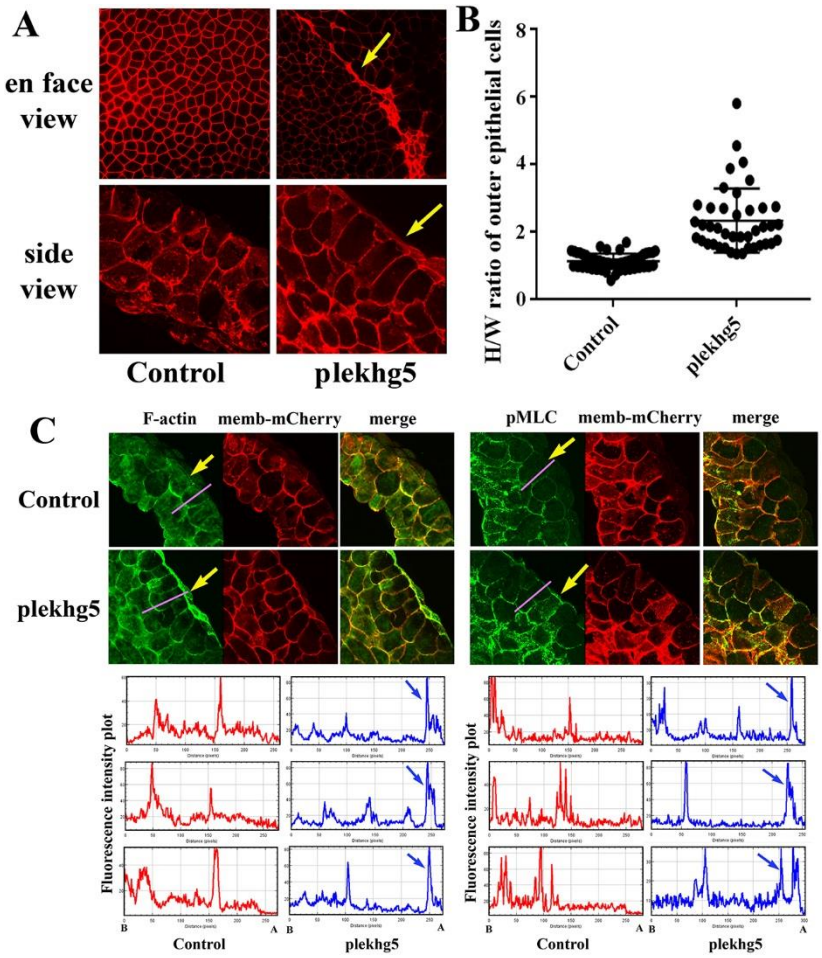

Figure 3. *plekhg5* induces cell elongation and apical actomyosin accumulation in outer epithelial cells. A) En face view of early gastrula embryos shows reduced cell surfaces in *plekhg5*-expressing cells (arrow) compared with those in control embryos; whereas side view of the bisected embryos shows elongation of superficial epithelial cells from *plekhg5*-injected embryos. B) Height (H) over apical width (W) ratio analysis shows that *plekhg5*-expressing outer epithelial cells have a significant increase in H/W ratio from 1.2 in control cells to 2.2 in *plekhg5*-expressing cells, with the p-value of 8.3E-21. C) *plekhg5* stimulates apical accumulation of both F-actin and phosphorylated myosin regulatory light chain (pMLC). The membrane-mCherry signal is used to label the injected cells. Arrows point to the apical F-actin and pMLC signals. Fluorescence intensity is measured with the NIH ImageJ program along the axis indicated by the line across the animal regions. The plots for three different biological samples are shown with the apical (A) and basal (B) direction labeled at the bottom. Blue arrows point to the apical enhancement of F-actin and pMLC signals.

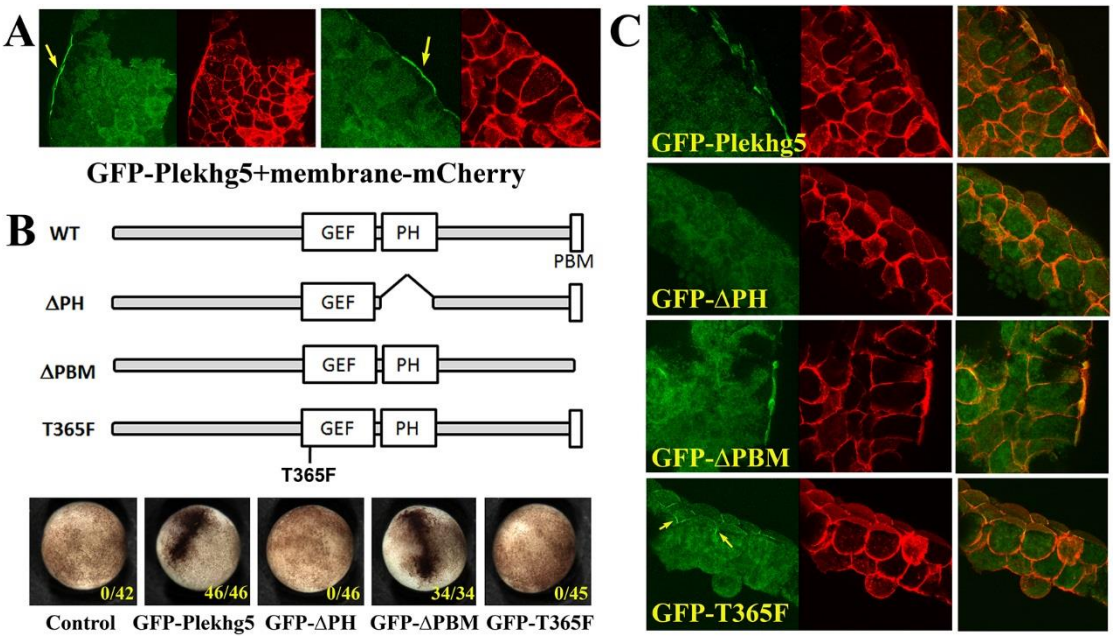

Figure 4. Plekhg5 is apically localized in the superficial epithelial cells. A) GFP-tagged Plekhg5 protein is detected at the apical cell cortex in the superficial epithelial cells (arrows), but is diffuse in deeper ectodermal cells. B) Plekhg5 contains a pleckstrin homology (PH) domain and a PDZ-binding motif (PBM) in addition to the GEF domain. Analyses of the deletion mutants that lack one of these domains reveal that removal of the PH domain, but not the PBM motif, abolishes the ability of the protein to induce ectopic blastopore lip. In addition, a point mutation that alters the conserved T365 residue in the GEF domain into F also results in non-functional Plekhg5. The number of the embryos with ectopic blastopore lip-like morphology over the total injected embryos is shown in the panels. C) Deletion of the PH, but not the PBM, domain results in loss of apical accumulation of the proteins. The T365F GEF mutant protein can be recruited to the cell junctions in epithelial cells (arrows), but is not enriched at the apical cell cortex.

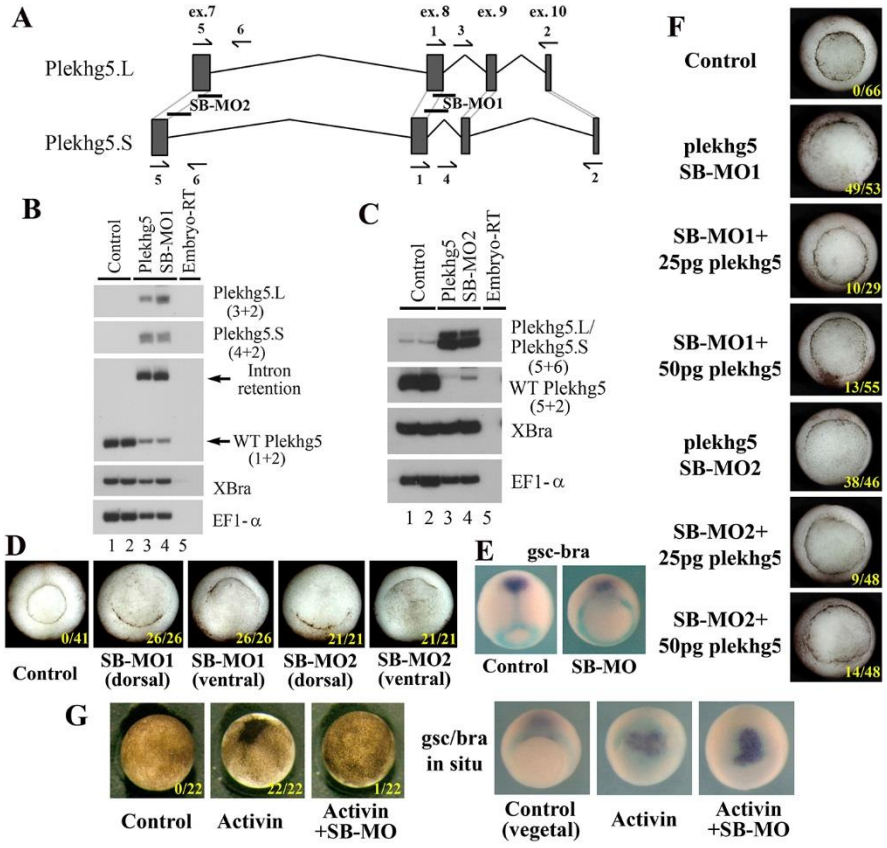

Figure 5. *plekhg5* is required for endogenous blastopore lip formation. A) Schematic representation of the genomic regions of the L and the S alloalleles of *plekhg5* that are targeted by the SB MOs. The positions of the primers used for RT-PCR analysis of splicing efficiency are shown. B, C) Both SB-MO1 and SB-MO2 efficiently block splicing of both L and S alloalleles, as indicated by the presence of intron-retention products in *plekhg5* morphant embryos. The primer pairs used in the PCR reactions are indicated in the parentheses. D) *plekhg5* SB-MOs prevent formation of the blastopore lip at the sites of its injection. E) *plekhg5* SB MOs do not alter mesodermal cell fates, though the movements of the prechordal tissue (*gsc*-expressing) and the trunk mesoderm (*bra*-expressing) are affected. F) The blastopore lip defects induced by the SB MOs (25ng) can be rescued with low doses of co-expressed *plekhg5* RNA (25-50pg). G) *plekhg5* SB MOs (25ng) block ectopic blastopore lip induction by activin (5pg) without affecting activin-dependent mesodermal induction. The numbers of the embryos with blastopore lip defects or ectopic blastopore lips over the total injected embryos are shown in the panels.

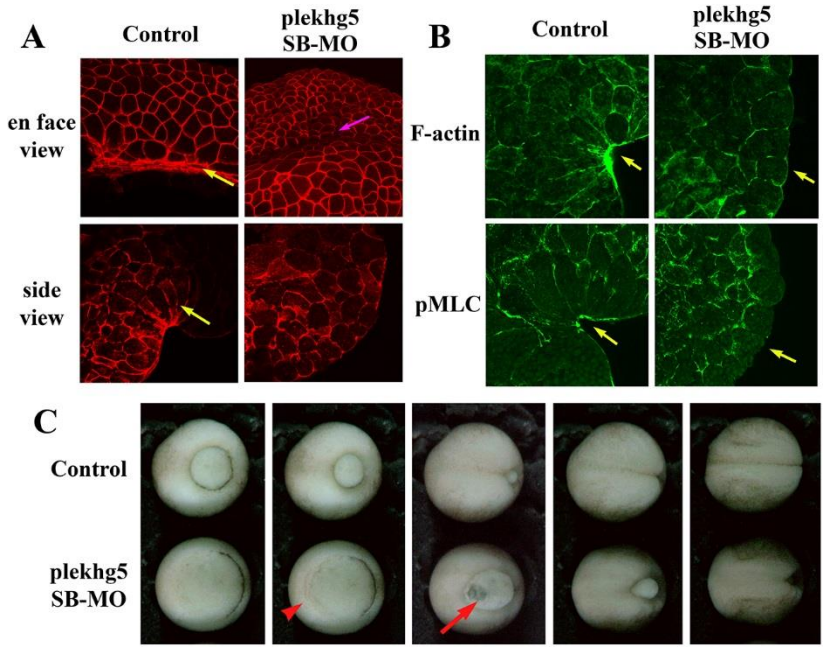

Figure 6. *plekhg5* regulates apical actomyosin cytoskeleton in bottle cells and gastrulation movements. A) En face and side views of control bottle cells show reduced cell surfaces and wedge-shaped morphology in gastrula embryos, respectively (yellow arrows). However, in *plekhg5* morphant embryos, cells do not show great shrinkage of surface areas and only cuboidal epithelial cell shapes are seen from the side view. Despite this, internalization of surface cells seems to happen at imprecise positions in the morphant embryos, as shown by formation of a surface groove (pink arrow). B) Both F-actin and pMLC are enriched in the apical cell cortex of the bottle cells in bisected control embryos, but no such enrichment is observed in *plekhg5* morphant embryos. Yellow arrows point to the apical signals. C) Gastrulation movements proceed in the absence of the bottle cells, as seen by accumulation of cells in the marginal region from epiboly (red arrowhead) and thinning of the vegetal mass due to rotational movements of the large endodermal cells upward and laterally (red arrow). Blastopore eventually closes at a delayed time in most morphant embryos when their control siblings reach the neurula stages. Selected still frames from a time lapse video of gastrulating control and *plekhg5* morphant embryos are shown here.

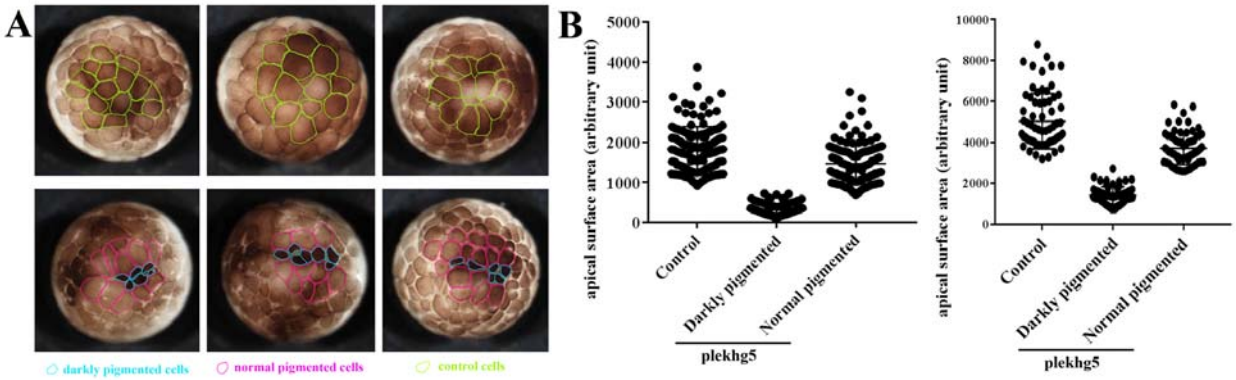

Fig. S1. Quantitative analysis of apical cell surface area in control and *plekhg5*-injected blastula embryos. A) Individual animal cells at the blastula stages were marked and their surface areas were measured using the NIH ImageJ software. B) Scatter plots of two individual experiments with mean and standard deviation are shown. GraphPad Prism7 software was used for the plot. Student t-test was also performed and showed that the differences between samples were significant.

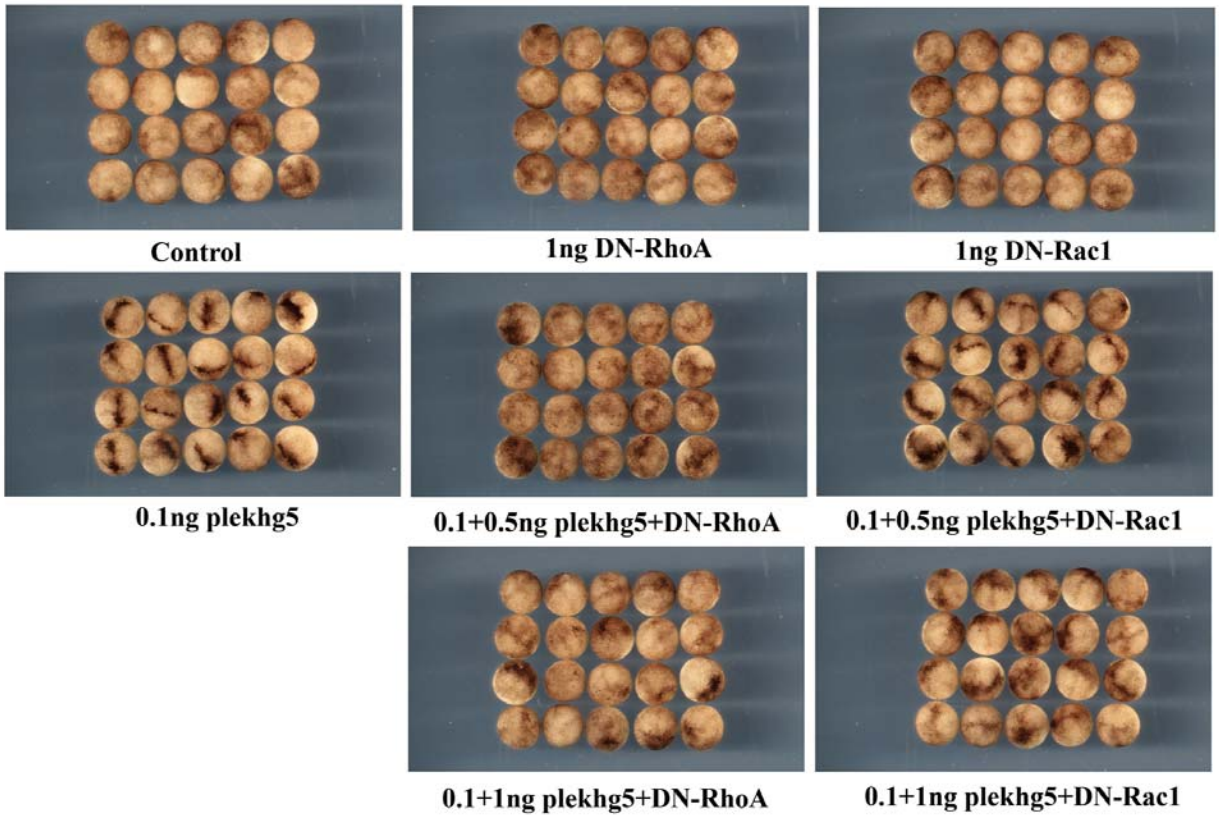

Fig. S2. Dominant negative (DN) RhoA, but not DN-Rac1, efficiently blocks ectopic blastopore lip induction by *plekhg5*. While expression of 1ng DN-RhoA or DN-Rac1 does not change animal cell morphology, 0.5ng to 1ng of DN-RhoA prevents ectopic blastopore lip-like morphology induced by *plekhg5*, whereas DN-Rac1 is not effective in inhibiting *plekhg5*.

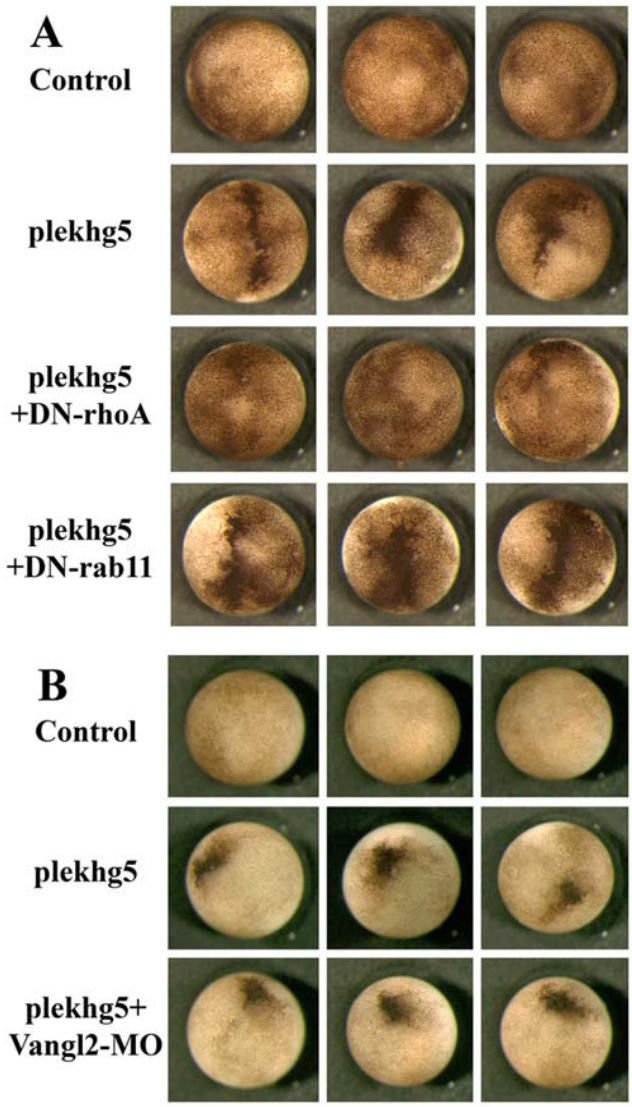

Fig. S3. Unlike DN-rhoA, neither DN-Rab11 (panel A), nor Vangl2-MO (panel B), blocks ectopic blastopore lip-like morphology by plekhg5. *plekhg5* RNA, 0.1ng, 22/22 embryos with ectopic blastopore lip; with DN-rhoA, 1-2ng, 2/23; with DN-Rab11, 1-2ng, 34/35; with Vangl2-MO, 25ng, 18/18 embryos.

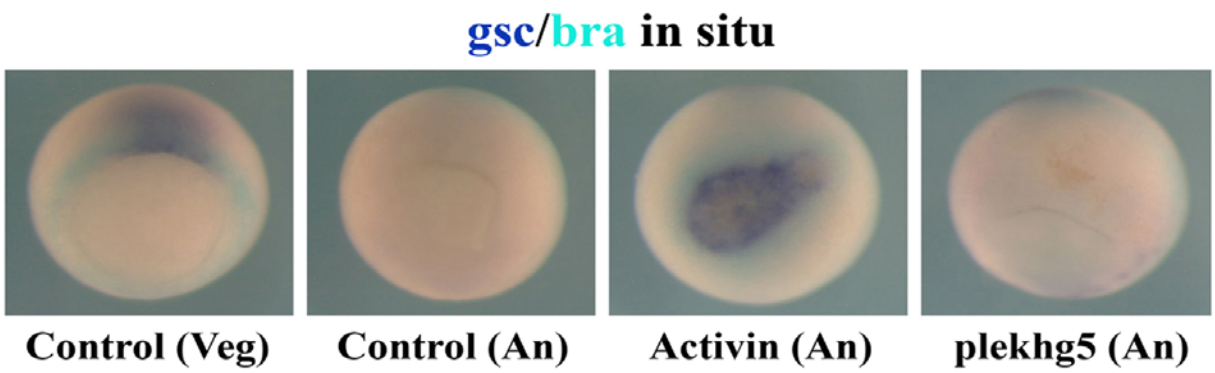

Fig. S4. Unlike activin, *plekhg5* does not induce the mesodermal markers gsc (*goosecoid*) and *bra* (*brachyury*) in the animal region. The vegetal view (Veg) of the left panel *shows* the endogenous expression of the mesodermal markers, and the animal view (An) of the other panels shows the ectopic expression of the markers.

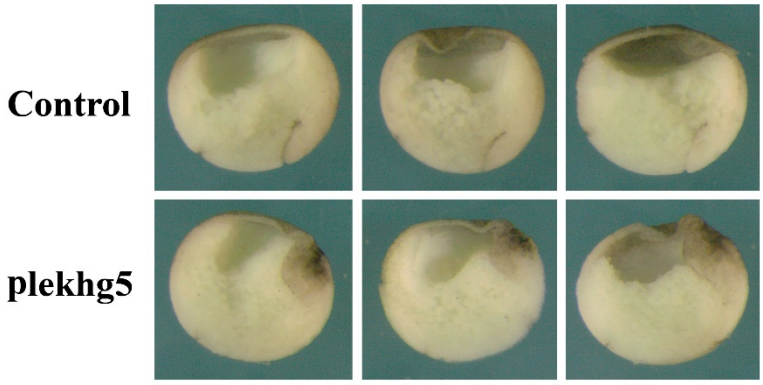

Fig. S5. *Plekhg5* interferes with radial cell intercalation in the ectoderm. Side view of bisected embryos reveals that ectopic expression of *plekhg5* blocks radial cell intercalation, resulting in thick mass of multi-layered cells underneath the darkly pigmented, apically constricting, superficial epithelial cells.

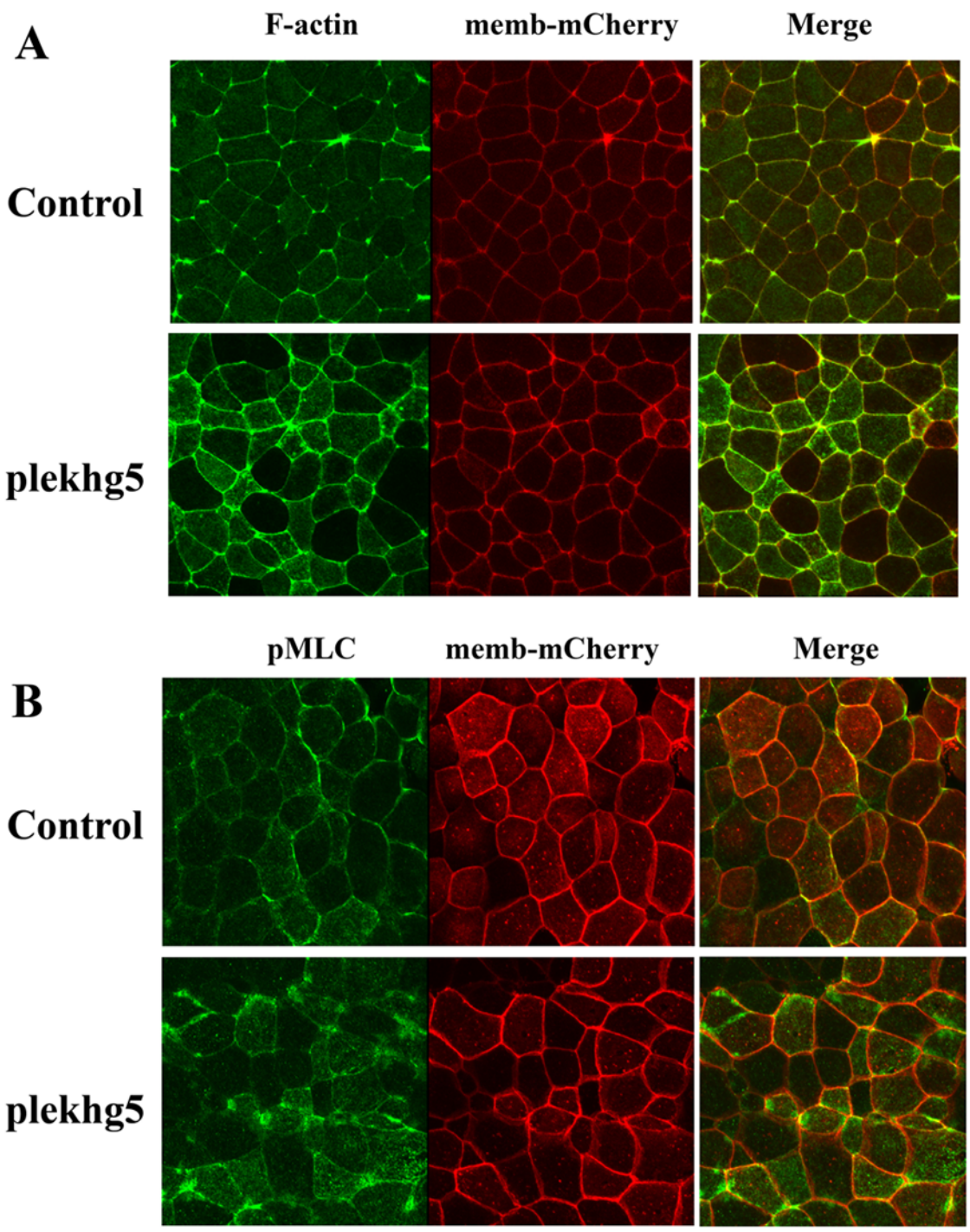

Fig. S6. *plekhg5* induces apical accumulation of F-actin and pMLC. En face view of the animal cells from the control or the *plekhg5*-injected embryos shows that both F-actin and pMLC preferentially localize to the cell junctions in control embryos, but their signals are enhanced at the apical cortex in *plekhg5*-injected embryos.

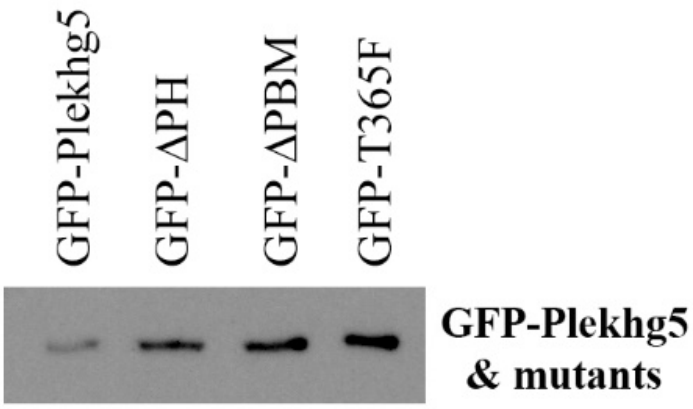

Fig. S7. Western blot analysis shows that GFP-Plekhg5 mutants are expressed at similar levels as GFP-Plekhg5.

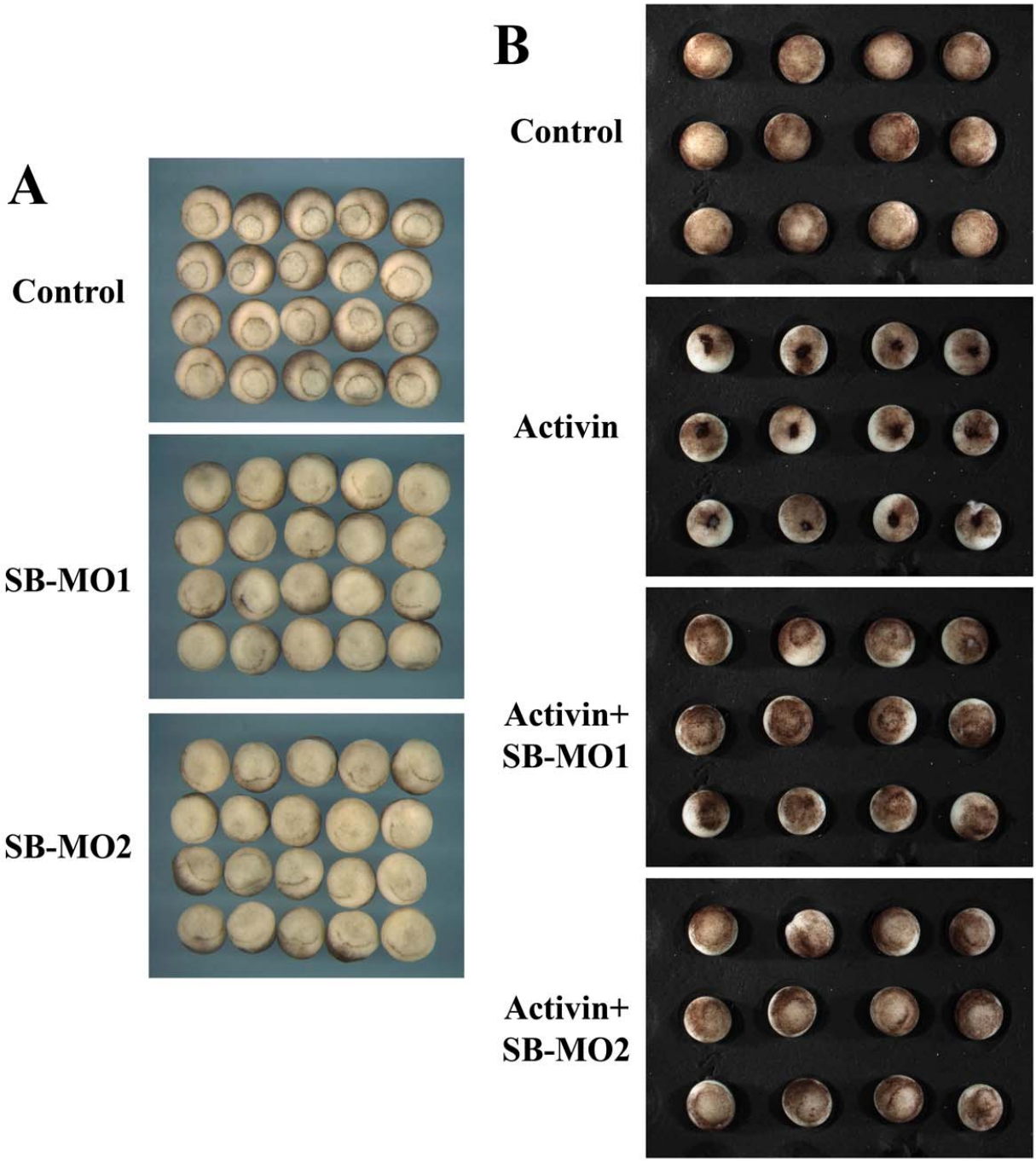

Fig. S8. Both *plekhg5* SB-MOs induce similar phenotypes in early Xenopus embryos. A) Injection of either SB-MO1 or SB-MO2 into the marginal zone region of early Xenopus embryos leads to defects in blastopore lip formation. B) Both *plekhg5* SB-MO1 and SB-MO2 block the ectopic blastopore lip induction by activin. Doses of reagents used: SB-MO1 and SB-MO2, 50ng; activin, 5pg.

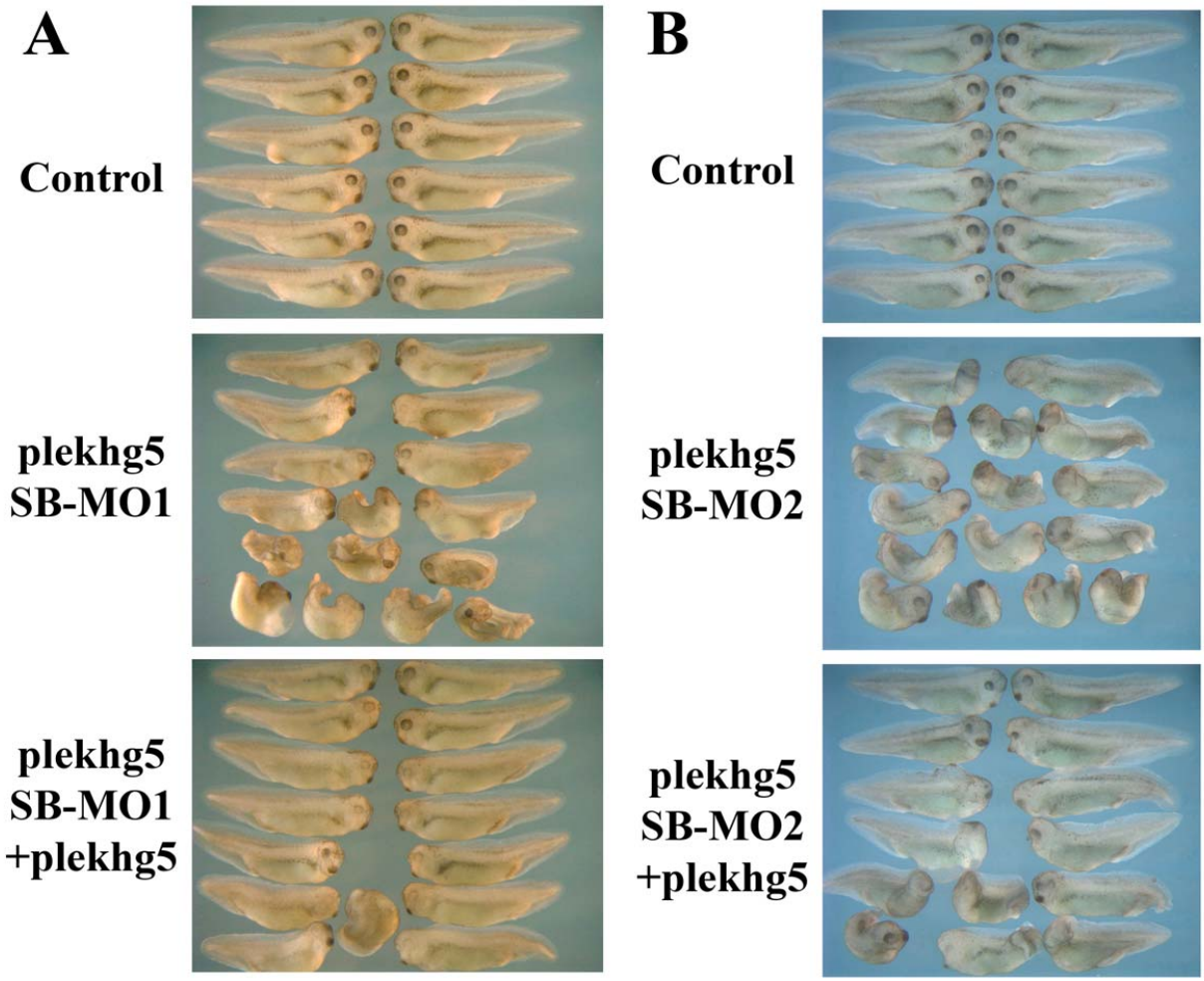

Fig. S9. *plekhg5* SB MOs induce axial defects at the tadpole stages that are largely rescued by co-expressed wild type *plekhg5* RNA. *plekhg5* SB-MOs (50ng) induce axial defects, including small head, shortened axis, and some with failure in blastopore closure. The defects are largely rescued when SB-MOs are co-expressed with wild type *plekhkg5* RNA (25-100pg).

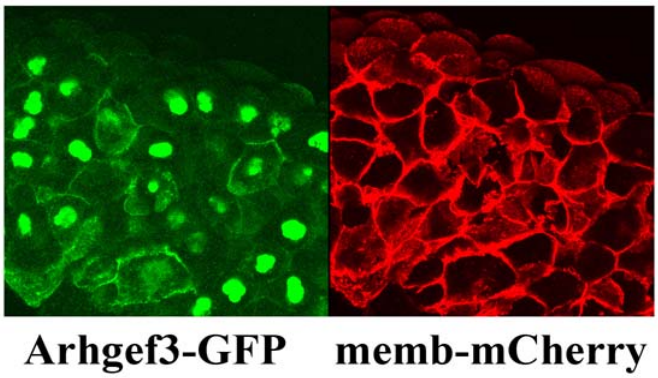

Fig. S10. Arhgef3, another organizer-enriched, PH-domain-containing RhoGEF, is localized strongly in the cell nucleus in addition to some membrane signals.

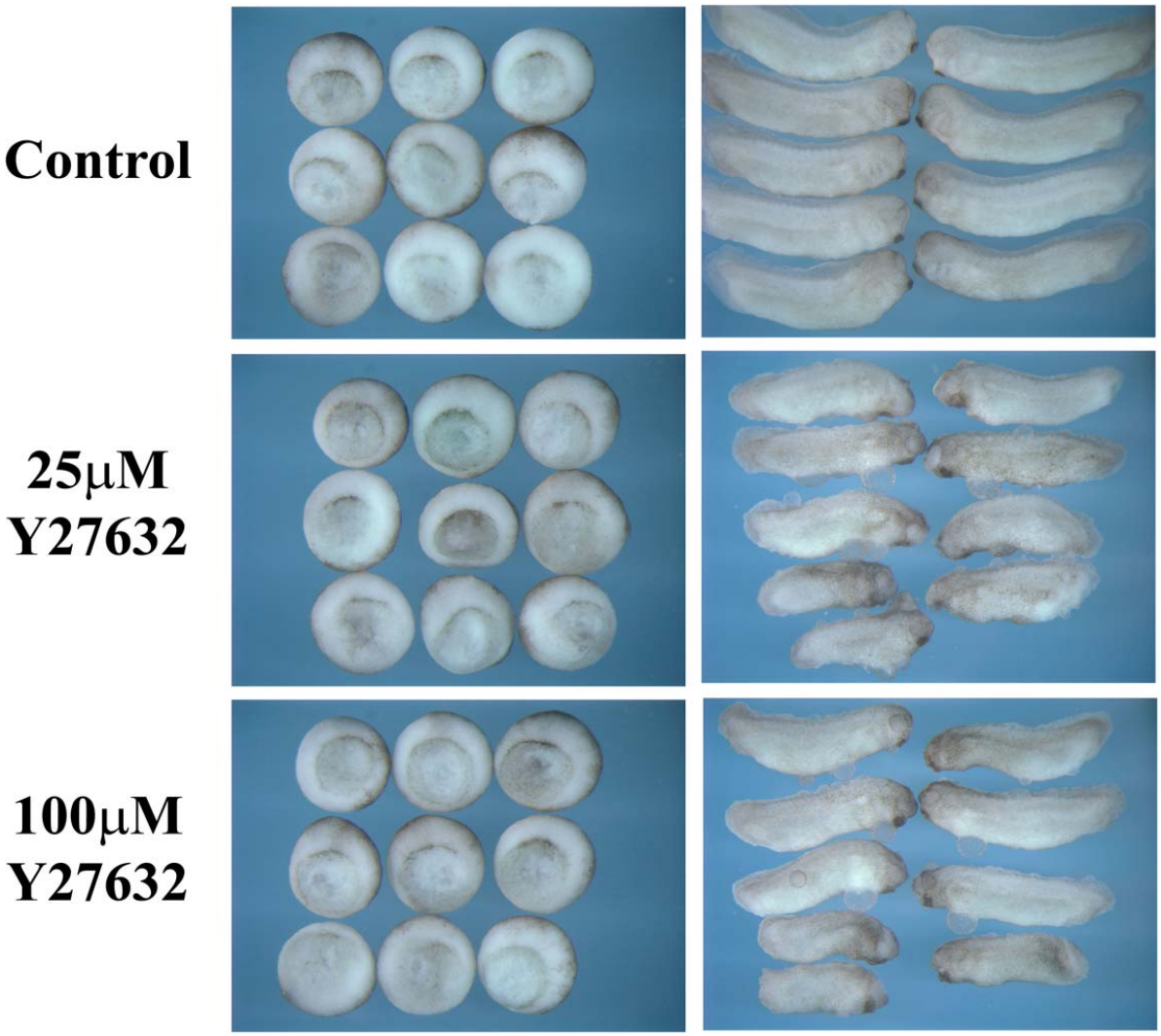

Fig. S11. Treatment of the blastula embryos with the ROCK inhibitor Y27632 does not prevent formation of the blastopore lip, though the embryos display multiple defects at later stages, including smaller head and skin blistering.

Movie 1. *plekhg5* induces apical constriction at blastula stages (embryo on the right), whereas activin induces ectopic blastopore lip only during gastrulation (embryo in the center). The control embryo is shown on the left.

Movie 2. Gastrulation movements in embryos with altered levels of *plekhg5*. The control embryo is shown on the left, the morphant embryo with *plekhg5* SB-MO injected into the dorsal marginal zone is shown in the center, and the embryo injected with the *plekhg5* RNA is shown on the right.

Movie 3. Injection of *plekhg5* SB-MO into the marginal zone of all 4 blastomeres at the 4-cell stages results in minimal blastopore lip formation during gastrulation. The embryos nonetheless accomplish blastopore closure when control siblings reach the neurula stages. Convergent extension tissue movements seem to drive the blastopore closure in the morphant embryos. Top two embryos are the controls and the bottom two embryos are the morphants.

Movie 4. Gastrulation movements of *plekhg5* morphant embryos with the MO injected either into the dorsal (left embryo) or the ventral (right embryo) side. The dorsally injected embryo shows defects in blastopore closure. This happens in a minority of the morphant embryos, suggesting a lack of precision in cell movements during gastrulation.